

This is a repository copy of *Competing Pathways in the Photochemistry of Ru(H)₂(CO)(PPh₃)₃*.

White Rose Research Online URL for this paper:

<https://eprints.whiterose.ac.uk/126914/>

Version: Accepted Version

Article:

Procacci, Barbara orcid.org/0000-0001-7044-0560, Duckett, Simon B. orcid.org/0000-0002-9788-6615, George, Michael W. et al. (6 more authors) (2018) *Competing Pathways in the Photochemistry of Ru(H)₂(CO)(PPh₃)₃*. *Organometallics*. om-2017-00802b.R1. pp. 855-868. ISSN 0276-7333

<https://doi.org/10.1021/acs.organomet.7b00802>

Reuse

Items deposited in White Rose Research Online are protected by copyright, with all rights reserved unless indicated otherwise. They may be downloaded and/or printed for private study, or other acts as permitted by national copyright laws. The publisher or other rights holders may allow further reproduction and re-use of the full text version. This is indicated by the licence information on the White Rose Research Online record for the item.

Takedown

If you consider content in White Rose Research Online to be in breach of UK law, please notify us by emailing eprints@whiterose.ac.uk including the URL of the record and the reason for the withdrawal request.

This document is confidential and is proprietary to the American Chemical Society and its authors. Do not copy or disclose without written permission. If you have received this item in error, notify the sender and delete all copies.

Competing pathways in the photochemistry of $\text{Ru}(\text{H})_2(\text{CO})(\text{PPh}_3)_3$

Journal:	<i>Organometallics</i>
Manuscript ID	om-2017-00802b.R1
Manuscript Type:	Article
Date Submitted by the Author:	n/a
Complete List of Authors:	Procacci, Barbara; University of York, Department of Chemistry Duckett, Simon; University of York, Chemistry George, Michael; Nottingham, Chemistry Hanson-Heine, Magnus; Nottingham, Chemistry Horvath, Raphael; University of Nottingham, School of Chemistry Perutz, Robin; University of York, Chemistry Sun, Xue Zhong; University of Nottingham, Chemistry Vuong, Khuong; UQ Dow Centre, School of Chemical Engineering Welch, Janet; University of York, Chemistry

SCHOLARONE™
Manuscripts

revised Dec 2017

Competing pathways in the photochemistry of $\text{Ru}(\text{H})_2(\text{CO})(\text{PPh}_3)_3$

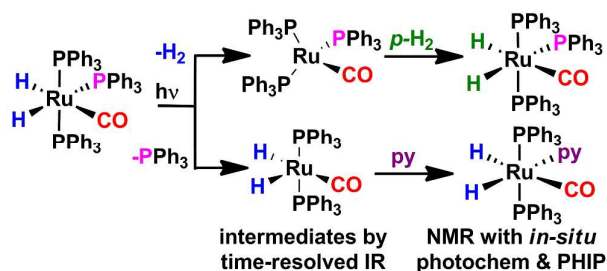
Barbara Procacci,^{1,2} Simon B. Duckett,^{*1,2} Michael W. George,^{*3,4} Magnus W. D. Hanson-Heine,³ Raphael Horvath,³ Robin N. Perutz,^{*1} Xue-Zhong Sun,³ Khuong Q. Vuong,³ and Janet A. Welch¹

1. Department of Chemistry, University of York, York YO10 5DD, UK

2. Centre for Hyperpolarisation in Magnetic Resonance, Department of Chemistry, York Science Park, University of York, York, YO10 5NY, UK

3. School of Chemistry, University of Nottingham, Nottingham NG7 2RD, UK

4. Department of Chemical and Environmental Engineering, The University of Nottingham Ningbo China, 199 Taikang East Road Ningbo 315100, China



Abstract

The photochemistry of $\text{Ru}(\text{H})_2(\text{CO})(\text{PPh}_3)_3$ **1** has been re-investigated employing laser and conventional light sources in conjunction with NMR spectroscopy and IR spectroscopy. The sensitivity of NMR experiments was enhanced by use of para- H_2 induced polarization (PHIP) and a series of unexpected reactions observed. The photo-induced reductive elimination of H_2 was demonstrated (a) *via* NMR spectroscopy by the observation of hyperpolarized **1** on pulsed laser photolysis in the presence of *p*- H_2 and (b) *via* nanosecond time-resolved infrared (TRIR) spectroscopy studies of the transient $[\text{Ru}(\text{CO})(\text{PPh}_3)_3]$. Elimination of H_2 competes with photo-induced loss of PPh_3 as demonstrated by formation of dihydrogen, triphenylarsine and pyridine substitution products which are detected by NMR spectroscopy. The corresponding coordinatively unsaturated 16-electron intermediate $[\text{Ru}(\text{H})_2(\text{CO})(\text{PPh}_3)_2]$ exists in two isomeric forms according to TRIR spectroscopy that react with H_2 and with pyridine on a nanosecond timescale. These two pathways, reductive elimination of H_2 and

1
2
3 PPh₃ loss are shown to occur with approximately equal quantum yields upon 355 nm
4 irradiation. Low-temperature photolysis in the presence of H₂ reveals the formation of the
5 dihydrogen complex Ru(H)₂(η²-H₂)(CO)(PPh₃)₂, which is detected by NMR and IR
6 spectroscopy. This complex reacts further within seconds at room temperature and its
7 behavior provides a rationale to explain the PHIP results. Furthermore, photolysis in the
8 presence of AsPh₃ and H₂ generates Ru(H)₂(AsPh₃)(CO)(PPh₃)₂. Two isomers of
9 Ru(H)₂(CO)(PPh₃)₂(pyridine) are formed according to NMR spectroscopy on initial photolysis
10 of **1** in the presence of pyridine under H₂. Two further isomers are formed as minor products;
11 the configuration of each isomer was identified by NMR spectroscopy. Laser pump-NMR
12 probe spectroscopy was used to observe coherent oscillations in the magnetization of the
13 one of the isomers of the pyridine complex; the oscillation frequency corresponds to the
14 difference in chemical shift between the hydride resonances. Pyridine substitution products
15 were also detected by TRIR spectroscopy.
16
17
18
19
20
21
22
23
24

25 Introduction

26
27 Photochemical methods offer low temperature routes to synthesis, excellent routes to study
28 reaction mechanisms and great opportunities for catalysis. Indeed, there has been a great
29 resurgence of interest in photocatalysis.¹⁻³ Metal hydrides play a major part in the
30 photochemistry of organometallics and coordination complexes and we have recently
31 reviewed their behavior systematically.⁴ One of the earliest metal hydrides to be studied
32 photochemically was Ru(H)₂(CO)(PPh₃)₃ **1** (Scheme 1), a compound of great interest for its
33 catalytic properties both under illumination and thermally.⁵⁻¹³ The original studies of its
34 photochemistry demonstrated loss of H₂, but not CO, on irradiation in benzene. Selectivity
35 for loss of H₂ over loss of CO is now recognized for several metal carbonyl dihydrides.¹⁴
36 When **1** was photolyzed in benzene solution under a CO atmosphere, Ru(CO)₃(PPh₃)₂ was
37 formed leaving the sequence in which H₂ and PPh₃ had been dissociated and CO
38 coordinated uncertain. In 1997, we identified **1** as an excellent target for investigating the
39 photodissociation of H₂ by time-resolved UV/vis and time-resolved IR spectroscopy.¹⁵ We
40 observed a transient by both techniques that was assigned to [Ru(CO)(PPh₃)₃] and
41 measured its rate of reaction with H₂ ((8.4 ± 0.4) × 10⁷ dm³ mol⁻¹ cm⁻¹ at room temperature).
42 It was of particular importance that the transient exhibited a 95 cm⁻¹ shift to low frequency in
43 its CO-stretching band, providing proof of H₂ loss. Moreover, ultrafast spectroscopy
44 demonstrated that it was formed within the response time of the instrument of 6 ps. The only
45 other transient observed by IR spectroscopy had a significant rise time suggesting that it was
46 a secondary product. Thus we concluded that there was ultrafast and concerted
47
48
49
50
51
52
53
54
55
56
57
58
59
60

1
2
3 photochemical reductive elimination of H₂ from Ru(H)₂(CO)(PPh₃)₃. As we now show, this
4 study failed to find evidence for a further process because of limitations of the methodology
5 and the techniques available to us at the time: neither the transient absorption nor the TRIR
6 experiments probed the timescale of 0.5 - 500 ns and our steady state NMR experiments
7 were conducted at room temperature and not at low temperature.
8
9

10 The advent of in-situ photochemistry at low temperature with NMR detection¹⁶⁻²⁵
11 offered a new method of probing reaction mechanism. In the case of a ruthenium complex
12 related to **1** in which one phosphine has been replaced by an N-heterocyclic carbene,
13 Ru(H)₂(IEt₂Me₂)(PPh₃)₂(CO) (IEt₂Me₂ = 1,3-bis(ethyl)-4,5-dimethylimidazol-2-ylidene), we
14 showed that, the products are actually consistent with two competing pathways, reductive
15 elimination of H₂ and dissociation of PPh₃.²⁶ Loss of PPh₃ was revealed by the formation of a
16 cyclometalation product in the absence of other substrates and
17 Ru(H)₂(IEt₂Me₂)(PPh₃)(CO)(L) (L = pyridine or η²-H₂) in the presence of H₂ or pyridine. The
18 combination of this photochemical technique with *para*-hydrogen induced polarization (PHIP)
19 showed weakly enhanced NMR resonances for the precursor and stronger enhancement for
20 two of its isomers. This effect could be understood by photoinduced reductive elimination of
21 H₂ followed by oxidative addition of *p*-H₂. Photochemical loss of phosphine competing with
22 loss of H₂ was also observed for Ru(H)₂(PMe₃)₄.²⁷ The timescales available and the
23 sensitivity of TRIR spectroscopy have improved greatly since our 1997 study and there are
24 no longer any gaps in the nanosecond time-domain.²⁸⁻³¹
25
26
27
28
29
30
31
32

33 Recently, we returned to the photochemistry of **1** and observed some unexpected
34 features in its reactivity towards *p*-H₂. We found that we could observe PHIP-enhanced
35 hydride resonances if we used a pulsed laser for excitation (at 355 nm) synchronized to the
36 NMR spectrometer under a pressure of *p*-H₂.³² Under these very dilute conditions with single
37 laser shots, there was negligible photodecomposition. Notably, the observed signal
38 enhancement decayed on a millisecond timescale and was only observed with
39 synchronization. This behavior was very different from that of related ruthenium complexes.
40 A paper published in 2017 has repeated these measurements with 308 nm irradiation and a
41 hydrogen pressure of 1 atm. The results are similar but some photodecomposition is
42 reported.³³
43
44
45
46

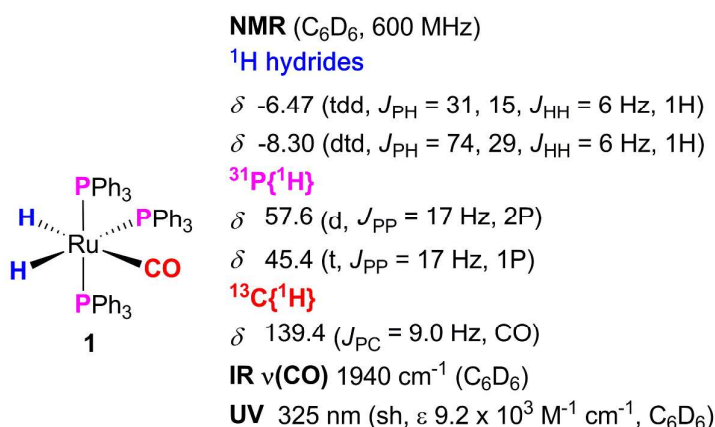
47 In this paper, we report a series of studies of the photochemistry of **1** by NMR and IR
48 methods; the NMR studies were performed using three types of experiment: (a) broadband
49 (λ > 290 nm) *ex-situ* irradiation, (b) continuous wave (cw) laser (λ = 325 nm) *in situ*
50 irradiation (NMR operating frequency 400 MHz); (c) pulsed laser (λ = 355 nm) *in situ*
51 irradiation (NMR operating frequency 600 MHz). The studies were conducted at
52 temperatures ranging from 220 -300 K. The infrared studies include time-resolved IR
53
54
55
56
57
58
59
60

spectroscopy at room temperature on timescales from nanoseconds to microseconds and FTIR methods at ca. 220 K. They reveal that photodissociation of PPh₃ occurs in addition to reductive elimination of H₂, leading to substitution products. We show that it is the interplay of these two pathways that limits the use of PHIP methods when applied to **1**.

Results

1. Characterization of Ru(H)₂(CO)(PPh₃)₃ **1 and detection of hyperpolarized **1**.** Complex **1** (Scheme 1) has been characterized previously^{15,34} but a summary of its main spectroscopic features are provided in Scheme 1 and a ¹H NMR spectrum of the key hydride region is illustrated in Figure 1a; a ³¹P{¹H} NMR spectrum is shown in the Supporting information.

Scheme 1. Structure of **1** and spectroscopic features.



When an optically dilute solution of **1** is irradiated with a single shot of the pulsed laser (355 nm) in the presence of *p*-H₂ (3 bar) and monitored through the response from a single, synchronized *r.f.* pulse that takes place up to 5 ms after laser irradiation, enhanced hydride signals at δ -6.47 and δ -8.30 are observed (Figure 1b). In this spectrum, J_{HH} corresponds to the peak separation of the antiphase features, while the other splittings arise from coupling to ³¹P nuclei.³² (The corresponding ¹H{³¹P} spectrum is shown in the SI). Similar hyperpolarization is observed on irradiation at 220 K. This result demonstrates that *p*-H₂ has been incorporated into **1**. Formation of hyperpolarized **1** can be understood by reductive elimination of H₂ upon 355 nm irradiation yielding [Ru(CO)(PPh₃)₃] which recombines with *p*-H₂ by oxidative addition. The re-addition of H₂ to [Ru(CO)(PPh₃)₃] is known to be fast under these conditions (the time constant for recombination under 3 atm H₂ is 1.4 μ s) precluding the detection of any transient species.

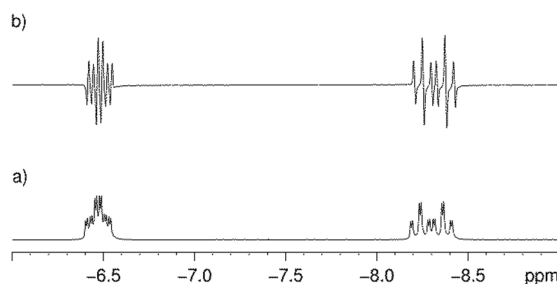


Figure 1. Hydride region of two ^1H NMR spectra of **1** in C_6D_6 after (a) 128 scans probing a concentrated solution of **1**; (b) one scan of an optically dilute solution after laser induced incorporation of $p\text{-H}_2$ yielding hyperpolarized hydride peaks; $\tau = 150 \mu\text{s}$.

2. NMR studies of the photochemistry of **1**. (a) Formation of $\text{Ru}(\text{H})_2(\eta^2\text{-H}_2)(\text{CO})(\text{PPh}_3)_2$,

2. In contrast to the measurements described above, the steady-state photolysis of an optically dilute solution of **1** under a $p\text{-H}_2$ atmosphere at 295 K in benzene- d_6 or toluene- d_8 undertaken either ex-situ ($\lambda > 290 \text{ nm}$) or in situ with a laser ($\lambda = 325 \text{ nm}$, cw) resulted in no change in the observed NMR spectra of these solutions and PHIP was no longer observed in the hydride resonances of **1**. Notably, a very intense peak for *ortho*- H_2 was visible before irradiation was initiated indicating consumption of $p\text{-H}_2$ via a thermal route.

When the in situ irradiation process with $p\text{-H}_2$ was repeated at 223 K (toluene- d_8), there was still no PHIP enhancement of **1** upon photolysis (2 min, $\lambda = 325 \text{ nm}$). However, a new broad resonance (fwhm ca. 63 Hz at 400 MHz) was observed at $\delta -5.82$ in the ^1H NMR spectrum along with new signals in the aromatic region indicating productive photochemistry and the formation of a new species **2** (Figure 2a).

The $^{31}\text{P}\{^1\text{H}\}$ NMR spectrum now displayed two new singlets at $\delta -6.0$ and $\delta 59.4$ in addition to the resonances of **1**. The new $^{31}\text{P}\{^1\text{H}\}$ peak resonating at $\delta -6.0$ was identified as free PPh_3 , and an experiment with inverse-gated decoupling (quantitative phosphorus) showed that the integration ratio of the unknown peak to the free PPh_3 is 2:1, suggesting that **2** contains two equivalent PPh_3 ligands (Figure 2b). Further cooling to 193 K resulted in no change in these NMR features; however, warming to 295 K led to the disappearance of these signals and reformation of **1**. Complex **2** could also be generated at low temperatures with pulsed laser irradiation ($\lambda = 355 \text{ nm}$, 48 laser shots, 10 Hz repetition rate). On the basis of these results, we assign **2** as the dihydrogen complex $\text{Ru}(\text{H})_2(\eta^2\text{-H}_2)(\text{CO})(\text{PPh}_3)_2$ formed by photochemically induced PPh_3 loss from **1** and coordination of H_2 (Scheme 2). Upon cooling to 193 K the associated NMR spectra of **2** show minimal change. Moreover, when a $\{^{31}\text{P}\}^1\text{H}$ NMR spectrum was recorded at 220 K using a broadband decoupling sequence, the peak for **2** remained unaltered whereas the resonances for **1** simplified to doublets retaining

only J_{HH} of 6 Hz between the two hydrides. These observations are fully consistent with rapid exchange between hydride and dihydrogen ligands in conjunction with quick relaxation and the averaging of hydride-phosphorus couplings to a small and hence invisible value. The exchange is likely to occur by the σ -CAM mechanism,³⁵ as has been shown in detail by Crabtree.³⁶ Furthermore, the disappearance of **2** upon warming is consistent with the well-known lability of dihydrogen as a two electron donor ligand.³⁷ Complex **2** is an analogue of $\text{Ru}(\text{H})_2(\eta^2\text{-H}_2)(\text{PPh}_3)_3$ formed from $\text{Ru}(\text{H})_2(\text{PPh}_3)_4$ thermally and is also closely related to $[\text{Ru}(\text{IPr})_2(\text{CO})(\eta^2\text{-H}_2)\text{H}]\text{BARF}_4$ (IPr = 1,3-bis(2,6-diisopropylphenyl)imidazol-2-ylidene).^{38,39,40} Comparisons may also be made to Ru and Ir complexes studied with partial deuteration.^{41,42}

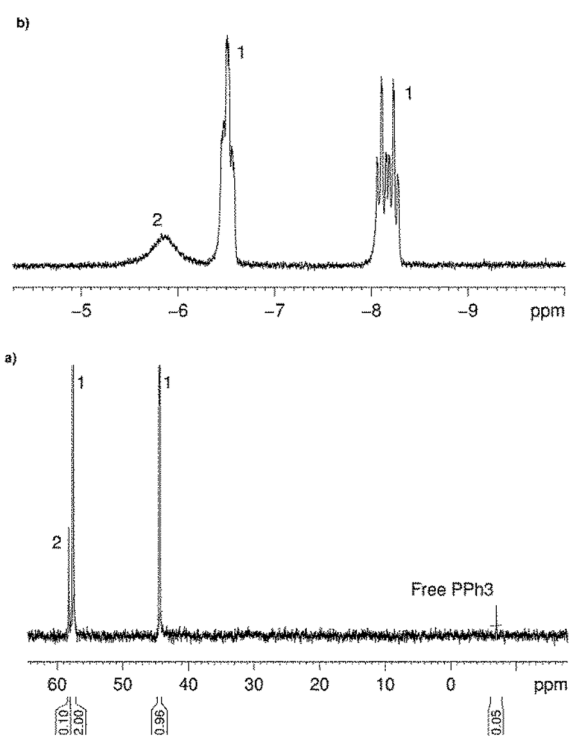
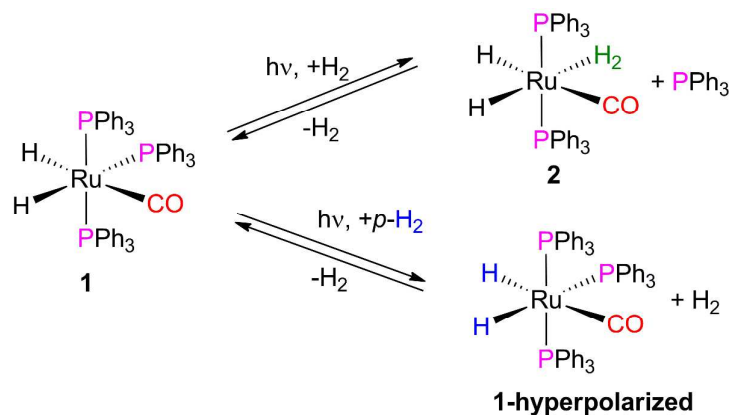


Figure 2. NMR spectra after the photolysis of **1** under $p\text{-H}_2$ in toluene- d_8 at 220 K. a) $^{31}\text{P}\{^1\text{H}\}$ NMR spectrum showing the formation of **2** and free PPh_3 . b) Hydride region of the ^1H spectrum displaying signals for **1** and a broad resonance for **2**.

Scheme 2. Competing photochemistry of **1** under H_2 atmosphere.



In order to confirm the presence of a dihydrogen ligand in **2**, data for T_1 were recorded at 400 MHz between 212 and 242 K for the resonance at $\delta -5.82$. The value of $T_{1(\text{min})}$ for **2** proved to be 35 ± 2 ms at ca. 225 K, whereas the corresponding value of T_1 for the hydride resonances of **1** was much longer (390 ms at 298 K). This is consistent with a dihydrogen arrangement as such ligands are known to relax much faster than their hydride analogues.^{37,43} Further analysis of the T_1 values is given in the Supporting Information.

We have already shown that PHIP was observed for the hydride resonances of **1** when a solution of **1** (C_6D_6) under $p\text{-H}_2$ (~4 bar) was irradiated at 298 K with a pulsed laser (355 nm) synchronized to the spectrometer.³² However, if this sample was irradiated with multiple laser shots (4 sets of 32 laser shots, 10 Hz repetition rate – 1 NMR scan), **2** was detected, although its signal disappeared after the first NMR scan due to its low stability. As complex **2** disappeared, the signals for **1** and a new hydride resonance start to grow in a thermal reaction. This new product signal appears at $\delta -6.34$, as a triplet with $J = 23$ Hz, that connects to a single $^{31}\text{P}\{^1\text{H}\}$ resonance at $\delta 57.1$ and simplifies into a singlet upon ^{31}P decoupling; it is assigned to known $\text{Ru}(\text{H})_2(\text{PPh}_3)_2(\text{CO})_2$.^{44,45}

Additional evidence for formation of **2** was obtained by photolysis of **1** under a D_2 atmosphere at 298 K using either a pulsed or continuous laser. Depletion of the hydride signal for **1** during photolysis along with the appearance of peaks for H_2 ($\delta 4.46$ in C_6D_6 , s) and HD ($\delta 4.41$ in C_6D_6 , t, $J_{\text{HD}} = 43$ Hz). There was also evidence of partial deuteration of **1** through broadening of the hydride resonances. Direct reductive elimination accounts for formation of H_2 . HD is logically formed through loss of PPh_3 and initial η^2 -coordination of D_2 to form the deuterium analogue of **2** followed by intramolecular exchange with the hydride ligands to yield $\text{Ru}(\text{H})(\text{D})(\text{HD})(\text{CO})(\text{PPh}_3)_2$ and ultimately HD. Complex **1-d₂** was generated by a sequence of three cycles of photolysis of **1** under D_2 (3 atm), followed by replacement of the atmosphere by fresh D_2 and further photolysis. At this stage, no HD or hydride resonances for **1** could be detected. Photo-reaction (325 nm) of the preformed **1-d₂** with H_2 at 223 K was then followed by ^1H NMR and, as expected, the hydride signals of both **1** and **2**

1
2
3 were seen. Although this sample should contain partially deuterated **2**, no J_{HD} splitting was
4 observed, even at 193 K. The lack of a visible HD splitting is consistent with rapid exchange
5 between the hydride and dihydrogen ligands.³⁷
6

7 Although the two hydride ligand signals of **1** are distinct at room temperature,
8 heteronuclear NOESY experiments have previously demonstrated that **1** undergoes
9 intramolecular ligand exchange at 335 K where the two hydrides exchange with each other
10 as well as with the inequivalent phosphines.⁴⁶ The exchange was postulated to occur *via* a
11 trigonal twist mechanism, but alternative mechanisms involving dihydrogen isomers are also
12 possible.⁴⁷ We undertook a series of 1D EXSY experiments to probe for the thermal
13 exchange of **1** with free H₂ or free PPh₃. The two hydride peaks and free hydrogen peak
14 were monitored at mixing times between 50 and 800 ms in C₆D₆ solution. As expected, slow
15 intramolecular exchange between the two hydride resonances was observed at room
16 temperature and faster exchange at 333 K as previously reported,⁴⁶ but no exchange with
17 free H₂ was detected up to 333 K demonstrating that no thermal H₂ elimination occurs on the
18 EXSY timescale of ca. 1 s (see Supporting Information). In similar experiments, exchange
19 between free PPh₃ and the phosphine ligands was monitored at 333 K (see Supporting
20 Information). Once more, no intermolecular exchange was observed in agreement with the
21 literature.⁴⁶
22
23
24
25
26
27
28

29 The photoreactions of **1** under H₂ provide evidence for H₂ reductive elimination and re-
30 addition through PHIP of **1**; evidence for competing PPh₃ dissociation is seen *via* the
31 observation of **2** and the formation of HD on photolysis under D₂.
32
33

34 **(b) Formation of Ru(H)₂(AsPh₃)(CO)(PPh₃)₂, **3**.** In order to further probe the
35 phosphine loss pathway, a sample of **1** (C₆D₆) was prepared under *p*-H₂ (~4 bar) in the
36 presence of a 10 fold excess AsPh₃. A ¹H{³¹P} NMR spectrum measured prior to photolysis
37 revealed slight conversion of **1** into a new species **3** with two very weak hydride resonances
38 at δ -6.28 and δ -9.46 ($J_{\text{HH}} = 6$ Hz) and a new singlet in the ³¹P{¹H} spectrum at δ 58. When
39 the sample was exposed to a single laser shot at 295 K, the hydride resonances of both **1**
40 and **3** became PHIP-enhanced (Figure 3). The intensities of the new product peaks were
41 also found to increase on irradiation with more laser shots. These peaks are split into triplets
42 of antiphase doublets, in an overall 1:1 intensity ratio, in the ¹H NMR spectrum and simplify
43 into antiphase doublets upon ³¹P decoupling. The triplet splitting is due to coupling to two
44 equivalent ³¹P nuclei that lie *cis* to the hydrides (δ -6.28, $J_{\text{PH}} = 30$ Hz ; δ -9.46, $J_{\text{PH}} = 26$ Hz).
45 We therefore assign **3** to Ru(H)₂(AsPh₃)(CO)(PPh₃)₂, formed by PPh₃ loss and AsPh₃
46 coordination, with the geometry shown in Scheme 3. Free PPh₃ was detected in the ³¹P{¹H}
47 spectrum as expected. Some thermal loss of PPh₃ occurs as is evident from the presence of
48 a little **3** before irradiation. Additionally, these observations also confirm that photolysis
49
50
51
52
53
54
55
56
57
58
59
60

causes PPh₃ loss along with H₂ reductive elimination. Complex **3** is relatively stable and can still be detected at room temperature after the *p*-H₂ response has decayed.

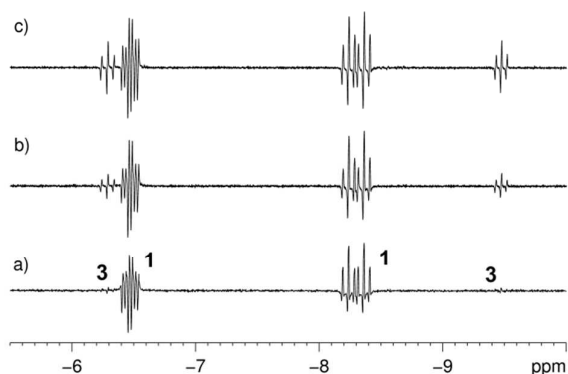
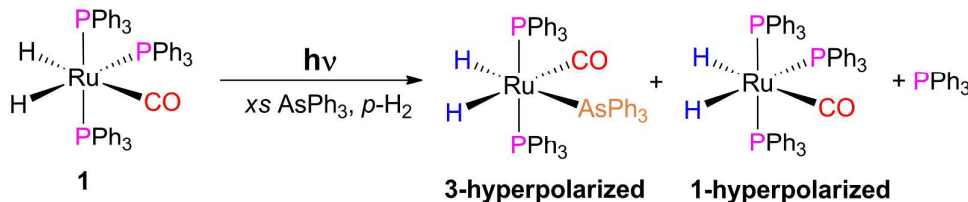


Figure 3. Hydride region of a series of ¹H NMR spectra of a solution of **1** in C₆D₆ in the presence of 10 fold excess AsPh₃ under *p*-H₂ at room temperature showing hyperpolarized signals for **1** and **3** after: a) 1 laser shot, b) 2 laser shots and c) 4 laser shots.

Scheme 3. Photochemistry of **1** in the presence of excess AsPh₃ and *p*-H₂.



(c) Formation of Ru(H)₂(CO)(PPh₃)₂(pyridine). An analogous reaction was then undertaken where AsPh₃ was replaced with pyridine. The thermal reaction of **1** with pyridine under *p*-H₂ (4 bar) at 298 K was first monitored in toluene-*d*₈ with added pyridine (10 μL). No reaction was observed by conventional NMR spectroscopy at 295 K; notably the presence of pyridine suppressed the conversion of *p*-H₂ to *o*-H₂ that had been observed in the absence of pyridine. However, when this process was repeated using the high sensitivity Only Para-hydrogen Spectroscopy (OPSY)⁴⁷ approach, two weak hydride resonances were observed that we assign to complex Ru(H)₂(CO)(PPh₃)₂(pyridine) **4-CN**. (We label the isomers of **4** according to the ligands that lie *trans* to the mutually *cis* hydride ligands. Thus **4-CN** indicates that the *cis* hydride ligands are *trans* to C and N, see below). Conversion to this product improved on increasing the temperature to 345 K, confirming a thermal route to its formation. The same product could be generated more efficiently by photochemical reaction in neat pyridine; after 3 h irradiation (λ > 290 nm, 295 K), 80% of the starting material **1** was converted to **4-CN** along with some minor by-products (see later).

1
2
3 The hydride region of the ^1H NMR spectrum, measured without hyperpolarization,
4 shows two major resonances for **4-CN** as triplet of doublets at $\delta -4.59$ ($J_{\text{PH}} = 27$ Hz, $J_{\text{HH}} =$
5 6.5 Hz) and $\delta -14.32$ ($J_{\text{PH}} = 23$ Hz, $J_{\text{HH}} = 6.5$ Hz) in a 1:1 ratio. These signals simplify into
6 doublets when ^{31}P is decoupled. The corresponding $^{31}\text{P}\{^1\text{H}\}$ NMR spectrum displayed a
7 singlet at $\delta 65.4$ for the main product. On the basis of these results we assign **4-CN** to
8 $\text{Ru}(\text{H})_2(\text{CO})(\text{PPh}_3)_2(\text{NC}_5\text{H}_5)$, an analogue of **3**, with mutually *trans* PPh_3 groups formed by
9 photochemical PPh_3 loss and reaction with pyridine. The hydride resonance at $\delta -14.32$
10 displayed a chemical shift characteristic of a hydride *trans* to nitrogen⁴⁸ while the remaining
11 hydride is assigned as *trans* to CO; free PPh_3 was also detected in the $^{31}\text{P}\{^1\text{H}\}$ spectrum.
12 Attempts to isolate **4-CN** were unsuccessful due to the lability of the pyridine ligand; when
13 the sample was pumped to dryness and redissolved in benzene, **1** was regenerated almost
14 quantitatively (see Supporting Information). When this reaction was repeated with a 10-fold
15 excess $\text{C}_5\text{D}_5\text{N}$ in benzene, the same product distribution was observed.

16
17 Irradiation of **1** in C_6D_6 under $p\text{-H}_2$ (4 bar) in the presence of 10 fold excess of pyridine-
18 d_5 with the pulsed laser at 295 K led to the detection of strongly hyperpolarized **1** (Figure 4a)
19 after a single laser shot with a single NMR scan.³² When the laser was allowed to fire two
20 shots consecutively (10 Hz repetition rate), PHIP-enhanced resonances of **4-CN** also
21 became visible after one NMR scan, observed as triplets of antiphase doublets in the ^1H
22 NMR spectrum. A weakly hyperpolarized resonance at $\delta -4.82$ with a shape that indicates a
23 product with an AA'XX' spin system was also observed (Figure 4b). We assign it to **4-PP**, an
24 isomer of **4-CN** with a square planar $\text{Ru}(\text{H})_2(\text{PPh}_3)_2$ skeleton where the two hydrides and two
25 phosphines are mutually *cis* (Scheme 4a). In this situation, the two hydrides are chemically
26 equivalent but magnetically inequivalent because of *cis* and *trans* phosphorus couplings,
27 which satisfies the symmetry-breaking conditions needed to detect PHIP. The ^{31}P resonance
28 of **4-PP** was found at $\delta 47.8$.

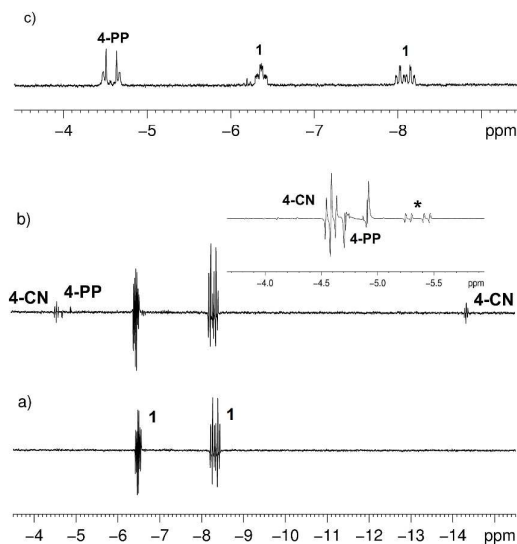
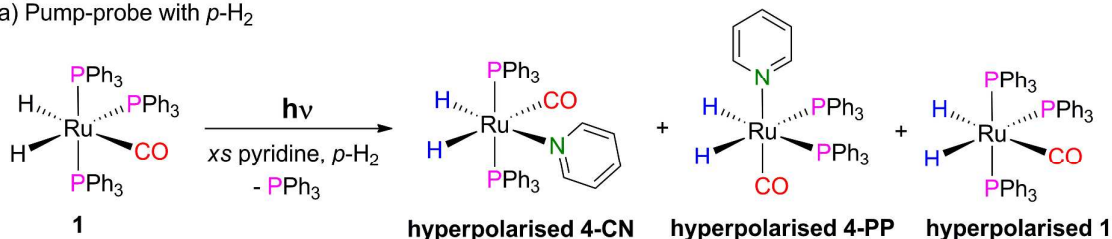


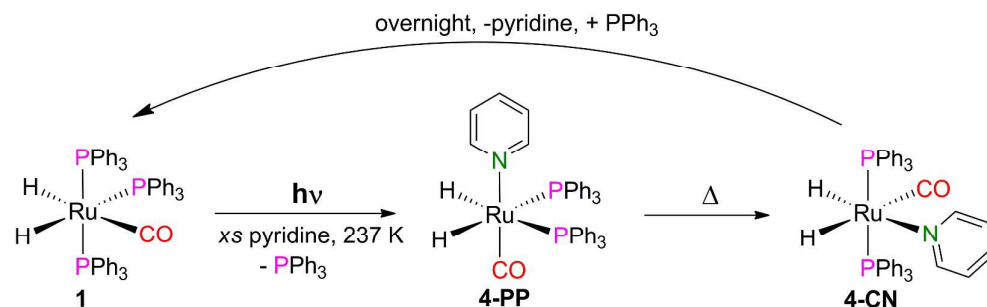
Figure 4. Hydride region of a series of ^1H spectra of **1** under $p\text{-H}_2$ in the presence of excess $\text{C}_5\text{D}_5\text{N}$ at room temperature. a) After a single laser shot in C_6D_6 solution showing hyperpolarized **1**; b) after two consecutive laser shots in C_6D_6 solution showing the formation of hyperpolarized **4-PP** and **4-CN**; Inset: expansion of the hydride peak for hyperpolarized **4-PP** (the inset spectrum was acquired with 4 laser shots; the doublet of antiphase doublets marked by an asterisk is due to another isomer **4-NP** see below) and c) spectrum acquired at 237 K in toluene- d_8 without hyperpolarization, showing signals for the primary photochemical product **4-PP** with a typical AA'XX' appearance (the change in chemical shift is due to use of a different solvent).

Scheme 4. Photoreactions of **1** with pyridine; (a) pump-probe photochemistry of **1** under p - H_2 atmosphere; (b) low-temperature photochemistry

(a) Pump-probe with p - H_2



(b) Low temperature photochemistry



The identities of **4-CN** and **4-PP** were confirmed by *in situ* irradiation of a C_6D_6 solution of **1** in the presence of 10 fold excess ^{15}N -pyridine under p - H_2 pressure with the pulsed laser. 1H - ^{15}N HMQC spectroscopy showed a cross peak between the hydride peak at δ – 14.32 for complex **4-CN** and a resonance at δ 270.4 in the ^{15}N spectrum which now exhibits a *trans* ^{15}N coupling of $J_{NH} = 12$ Hz (see Supporting Information). A cross peak was also observed between the hydride resonance for complex **4-PP** and a signal in the ^{15}N NMR spectrum at δ 256.3 indicating a small *cis* J_{NH} coupling (< 2 Hz).

The irradiation of a solution of **1** in C_6D_6 in the presence of 10 fold excess C_5D_5N under p - H_2 pressure at room temperature (Figure 5a) with 32 pulsed laser shots (355 nm, 10 Hz repetition rate) resulted in almost quantitative conversion to **4-CN** (Figure 5b). Given that we are only irradiating a small sample cross section but monitoring across the whole sample, we can confirm that diffusional mixing is rapid on this timescale in order to allow for the quantitative conversion. When this sample was shaken to refresh the dissolved p - H_2 to test thermal exchange between free H_2 and the hydrides of **4-CN**, PHIP was detected on the hydride resonances (Figure 5c) leading to the conclusion that the hydride ligands of the pyridine complex **4-CN** exchange thermally with free H_2 at room temperature. These observations contrast with the behavior of **1** for which no direct thermal exchange with free H_2 was observed at room temperature. When the same solution of **4-CN** is left overnight and checked again by NMR, quantitative regeneration of the starting complex **1** is observed highlighting the lability of the pyridine ligand which is slowly displaced by the stoichiometric

amount of PPh_3 present in solution after photosubstitution.

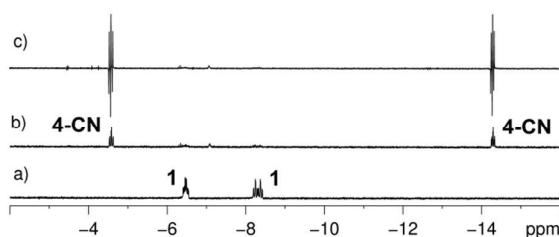


Figure 5. Hydride region of a series of ^1H NMR spectra of a solution of **1** in C_6D_6 in the presence of a 10 fold excess of $\text{C}_5\text{D}_5\text{N}$ under H_2 pressure at room temperature. a) Hydride resonances of **1** before laser irradiation; b) after 32 laser shots at 355 nm showing mainly **4-CN**; c) same sample after being shaken with $p\text{-H}_2$ that displays PHIP of **4-CN**.

The photoreaction of **1** with pyridine (10 μL) under $p\text{-H}_2$ was also studied with cw laser irradiation (325 nm) at 223 K in toluene- d_8 . Following photolysis (2 min), hyperpolarized signals were observed for **4-CN** and **4-PP** but not for **1**. (Note that no hyperpolarization of **1** is observed unless the pulsed laser is used and synchronized with the *r.f.* pulse of the spectrometer.) There was no evidence for the formation of **2** in these spectra, but the persistence of hyperpolarization after the photolysis source has been switched off confirms that **4-CN** and **4-PP** continue to undergo rapid thermal hydride ligand exchange with $p\text{-H}_2$ as demonstrated above.

In order to probe the isomerization of **4-CN** and **4-PP**, *in-situ* photolysis of **1** in neat $\text{C}_5\text{D}_5\text{N}$ was conducted at 237 K without a H_2 atmosphere. After 24 laser shots, 2.5% conversion was observed with the initial ratio of **4-PP** to **4-CN** being 2:1. Further photolysis increased the overall conversion level without change in the ratio of **4-PP** to **4-CN** (Figure 6). The proportion of **4-CN** increased, however, with increase in temperature suggesting thermal equilibration between the two isomers (Figure 7). When the solution was allowed to warm up to room temperature **4-PP** converted to **4-CN** quantitatively. Totally analogous behavior was found when the same experiment was repeated under a H_2 atmosphere (4 bar). Similarly, no changes in behavior were observed when the reaction was run in toluene- d_8 with 10-fold excess pyridine. These experiments lead to the surprising conclusion that **4-PP** is the first product of this reaction to be formed at low temperature that is stable on an NMR timescale, i.e. the primary photoproduct (Scheme 4b).

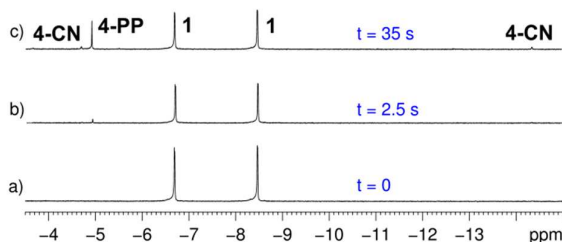


Figure 6. Hydride region of a series of $^1\text{H}\{^{31}\text{P}\}$ spectra of a solution of **1** in neat $\text{C}_5\text{D}_5\text{N}$ at 237 K. a) Starting solution at photolysis time = 0; b) after 2.5 s photolysis at 355 nm; c) after 35 s photolysis;

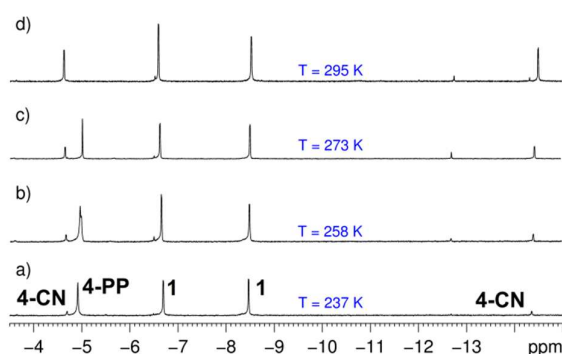


Figure 7. Hydride region of a series of $^1\text{H}\{^{31}\text{P}\}$ spectra of a solution of **1** in neat $\text{C}_5\text{D}_5\text{N}$ after 140 s of photolysis showing equilibration between **4-PP** and **4-CN** with increasing temperature. a) $T = 237$; b) $T = 258$ K; c) $T = 273$ K; d) $T = 295$ K.

We then used the PHIP effect to search for the formation of minor products in this reaction. When a sample of **1** under $p\text{-H}_2$ in C_6D_6 with a 10-fold excess of pyridine was exposed to multiple shots (up to 8) of the pulsed laser (355 nm) two new hyperpolarized minor species appeared in addition to those of **4-CN** and **4-PP** (Figure 8). Furthermore, under these higher signal-to-noise conditions hyperpolarization was clearly visible in the *ortho* aromatic protons of **4-PP** and the ^{31}P resonance of this complex at δ 47.8 (see Supporting Information). Analogous behavior has been observed before for a complex with chemically equivalent but magnetically inequivalent hydrides.³² The hydride resonances for the first of these species, complex **4-NP**, appear at δ -6.91 and -15.28 (Scheme 5). The hydride at δ -6.91 was assigned to lie *trans* to a PPh_3 group because of the large J_{PH} coupling (79 Hz, *cis* J_{PH} was measured as 40 Hz). The other hydride ligand of **4-NP** was detected by photochemical hyperpolarized COSY and assigned to lie *trans* to pyridine ($J_{\text{PH}} = 16, 30$ Hz, see Supporting Information for COSY). The second product, **4-CP**, exhibits a much weaker pair of hydride ligand signals whose chemical shifts and coupling constants

(δ -3.47; $J_{\text{PH}} = 23, 30$ Hz and -5.35 ; $J_{\text{PH}} = 32, 98$ Hz) indicated that one hydride is *trans* to CO and the other *trans* to PPh₃. With ¹⁵N labeled pyridine, a very weak cross peak between the hydride peak at δ -15.28 of complex **4-NP** and a signal in the ¹⁵N NMR spectrum at δ 266.2 was also detected ($J_{\text{NH}} = 14$ Hz) confirming that the pyridine lies *trans* to the hydride, as indicated by the characteristic chemical shift. No ¹⁵N-¹H cross peaks were observed for **4-CP**. A change of the solvent to neat pyridine did not provide additional information.

Scheme 5. Structures of the minor photolysis products with added pyridine.

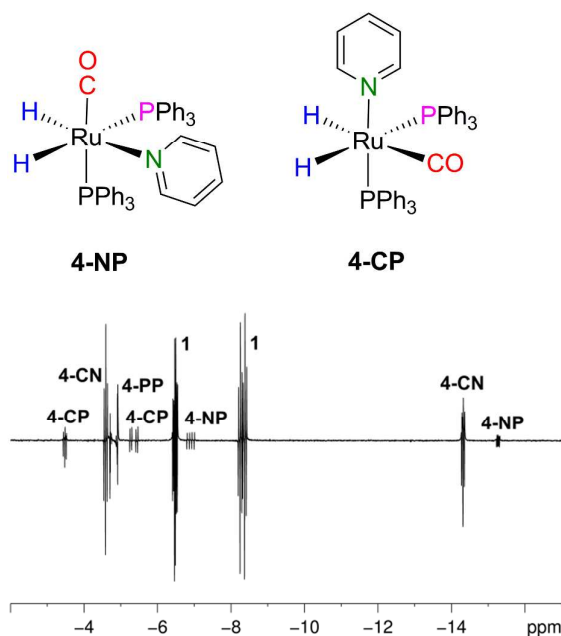
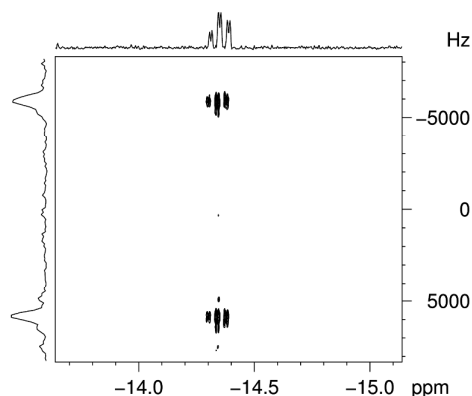


Figure 8. Hydride region of the hyperpolarized ¹H NMR spectrum of a C₆D₆ solution of **1** under *p*-H₂ in the presence of excess C₅D₅N. The solution was monitored after 8 laser shots.

In order to quantify the ratio of H₂ reductive elimination to PPh₃ loss, a sample of **1** was irradiated (355 nm) with the same concentration of D₂ and pyridine-*d*₅ (both 0.012 M, 10 fold excess) at 300 K. Under these conditions, H₂ loss is followed by D₂ oxidative addition to form **1-d₂**; loss of PPh₃ leads to conversion to pyridine complex **4-CN**. Pentafluoroanisole was used as an internal standard after ensuring that the compound was inert to it under these reaction conditions. ¹H NMR spectra were acquired at different photolysis time intervals; the reaction was taken to 50% conversion. The overall quantity of **1** and **1-d₂** was measured by integration of the *ortho* protons (12 H) (δ 7.46) for the axial phenyl rings of **1** that are well resolved. The integration of the hydride peak of **1** reported on the amount of **1** that remained undeuterated. The *ortho* protons (12 H) of **4-CN** (δ 7.94) quantified the production of **4-CN**.

1
2
3 Because of thermal exchange with D_2 (see above), the hydride resonances for complex **4-CN**
4 were not detected. This experiment established that at 50% conversion of **1**, H_2
5 reductive elimination accounts for $\leq 40\%$ of the photochemical reactivity while PPh_3 loss
6 takes place with 60% probability. We were concerned that under these conditions formation
7 of **2-d₂** could compete with formation of **4-CN** following loss of PPh_3 . We therefore repeated
8 the experiment under exactly the same conditions but with a large excess of pyridine with
9 respect to D_2 in order to turn formation of **2-d₂** into an uncompetitive route. Under these
10 conditions, the ratio of PPh_3 loss to H_2 reductive elimination products were 52:48. These
11 results indicate approximately the same quantum yields for the two photochemical
12 processes.
13
14
15
16
17

18 We have previously shown that it is possible to probe the hydride signal intensities
19 under hyperpolarization conditions in a series of NMR measurements recorded as a function
20 of the delay, τ , between the laser irradiation step and the *r.f.* pulse. When an optically dilute
21 solution of **1** in C_6D_6 is used and the appropriate laser energy applied there is no
22 decomposition of the sample due to photolysis, this allows the same solution to be used
23 multiple times. The response is expected to oscillate at the frequency difference between the
24 two coupled hydride resonances ($\Delta\nu$ in C_6D_6 9.75 ppm = 5851 Hz).^{32,49} The evolution of the
25 PHIP-enhanced NMR signals for **4-CN** was investigated in this way. A C_6D_6 solution of **1**
26 in the presence of excess pyridine under *p*- H_2 (4 bar) was therefore irradiated with the pulsed
27 laser (355 nm). The resonances of **1** oscillate in intensity as reported before. Analogous
28 coherent oscillations in intensity were found for the hydride resonances of **4-CN** at a
29 frequency of 5850 ± 5 Hz. Figure 9 illustrates the oscillation in the form of a 2D spectrum
30 fourier-transformed with respect to the pump-probe delay, τ .
31
32
33
34
35
36
37
38
39



40
41
42
43
44
45
46
47
48
49
50
51
52
53
54
55
56
57
58
59
60
Figure 9. 2D 1H pump-probe NMR spectrum of a C_6D_6 solution of **4-CN** where the vertical dimension corresponds to evolution frequency encoded by τ . Measurements are made with four laser pulses followed at delay τ by a single NMR pulse. Hydrides $\Delta\nu$ in C_6D_6 9.75 ppm =

5851 Hz, oscillation frequency 5850 ± 5 Hz.

The NMR results demonstrate clearly that two competing pathways occur during the photochemistry of complex **1**. One photochemical process is H₂ reductive elimination, as demonstrated by the observation of PHIP in the associated hydride peaks after irradiation under a *p*-H₂ atmosphere and incorporation of deuterium if photolyzed under a deuterium pressure. *In-situ* photolysis at low temperature led to the discovery of a competing photochemical pathway involving PPh₃ loss, first identified through the formation of the dihydrogen complex **2**. Subsequently, the triphenylarsine complex **3** and the pyridine complexes, **4-CN** and **4-PP** were formed without the need for low temperatures. We determined that quantum yields for H₂ reductive elimination and PPh₃ loss at 300 K to be approximately equal. The use of *p*-H₂ is critical to revealing some of these species. However, the formation of the dihydrogen complex **2** causes *p*-H₂ relaxation, but this conversion can be suppressed by addition of other ligands such as pyridine. We observed no Ru(0) products either at room temperature or low temperature. We therefore wished to know if evidence from TRIR spectroscopy is compatible with these conclusions.

2. IR studies. In the earlier experiments, the transient [Ru(PPh₃)₃(CO)] was detected by both time resolved UV-vis and IR spectroscopy of **1**, [$\lambda_{\text{max}} = 380$ nm, $\nu(\text{CO}) = 1845$ cm⁻¹] and found to react with H₂ to regenerate **1** on a microsecond timescale [$k_2 = (8.4 \pm 0.4) \times 10^7$ dm³ mol⁻¹s⁻¹]. The unsaturated species [Ru(PPh₃)₃(CO)] was found to be formed within 6 ps by ultrafast TRIR indicating that reductive elimination of H₂ also takes place on this timescale.¹⁵ Our new results suggested that it should also be possible to detect PPh₃ loss by TRIR spectroscopy. We have therefore undertaken new TRIR experiments with modern equipment with higher sensitivity and nanosecond time-resolution. We first report investigations of the photochemistry of **1** by low temperature FTIR spectroscopy.

(a) Photolysis of 1 monitored by FTIR spectroscopy. Figure 10a shows the IR difference spectra obtained following irradiation of a solution of **1** in toluene-*d*₈ at 220 K under Ar. The parent $\nu(\text{CO})$ band at 1937 cm⁻¹ is bleached and a new band at 1980 cm⁻¹ is formed. The band at 1980 cm⁻¹ can be assigned to a dimeric product, as was proposed in the previous TRIR studies.¹⁵

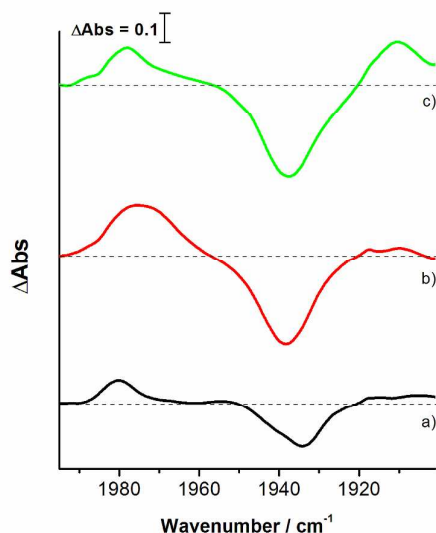


Figure 10. Difference spectra of **1** after photolysis at 220 K in toluene- d_8 (a) under argon; (b) under hydrogen (ca. 1 atm) (c) with added pyridine in toluene- d_8 (0.1 mL in 5.0 mL) under argon. The Δ Absorbance values have been normalized.

A similar experiment, performed under H_2 (1 atm), led to bleach of the parent band and the production of a broad band at ca. 1975 cm^{-1} (Figure 10b). These spectra were fitted using a multi-Lorentzian function indicating the presence of two overlapping bands at ca. 1980 and 1971 cm^{-1} . The solution was warmed up to 240 K and FTIR spectra were acquired every 3 min. The band at 1971 cm^{-1} decayed much faster than the 1980 cm^{-1} band providing further support for the presence of two bands. The band at 1971 cm^{-1} can be assigned to the hydride dihydrogen species **2** which arises from phosphine loss and reaction of the $[Ru(PPh_3)_2(CO)(H)_2]$ fragment with H_2 in agreement with the result from NMR spectroscopy.

The photolysis of **1** at 220 K was carried out in the presence of added pyridine in toluene under Ar and again the dimeric band was observed together with a new band at 1911 cm^{-1} (Figure 10c). We also carried out a similar experiment at room temperature in benzene with added pyridine- d_5 and observed the product at 1921 cm^{-1} (see SI). We assign the band at 1921 cm^{-1} to complex **4-CN** and the band at 1911 cm^{-1} observed at 220 K to **4-PP**, based on the isomer distribution observed by NMR spectroscopy.

TRIR spectroscopy. Earlier TRIR studies were conducted in C_6D_6 at room temperature and showed that H_2 elimination from **1** ($\nu(CO)$ 1940 cm^{-1}) formed the 16e⁻ Ru(0) species $[Ru(CO)(PPh_3)_3]$ with a $\nu(CO)$ band at 1840 cm^{-1} .¹⁵ These results were obtained covering a time window of 1 to 1000 μs employing a lower resolution instrument based on a CO laser.¹⁵ We have repeated these measurements using more sensitive instrumentation with faster time resolution. All the IR experiments were carried out in optically dilute solutions of **1** in C_6D_6 for consistency with the NMR experiments.

1
2
3 **TRIR of 1 under an Ar atmosphere in C₆D₆.** Figure 11 shows the TRIR difference
4 spectra at 298 K of **1** in C₆D₆ obtained at 1 ns (a) and 23 μs (b) following irradiation at 355
5 nm. The TRIR spectrum obtained after 1 ns shows bleach of the parent band and a product
6 band at 1840 cm⁻¹ (not shown in Figure 11) which was observed in the previous TRIR
7 experiments¹⁵ and can be assigned to the Ru(0) species [Ru(PPh₃)₃(CO)] arising from H₂
8 reductive elimination. Two new bands are also produced at ca. 1951 and 1911 cm⁻¹ which
9 were not observed in the previous TRIR measurements. The TRIR spectrum obtained 28 μs
10 after the flash shows that these two bands have decayed and a new absorption is formed
11 due to the dimeric product at 1971 cm⁻¹. The bands at 1951 and 1911 cm⁻¹ are tentatively
12 assigned to two different isomers of [Ru(PPh₃)₂(CO)H₂] produced by PPh₃ loss. These
13 bands decay with two components, a fast component (1.7 ns) that approximately matches
14 rapid reformation of the parent (ca. 4 ns, a,b) and a slower decay (ca. 10 μs, c,d) which is
15 similar to the formation of the dimeric band and the further bleaching of the parent. The
16 precise nature of the fast component is not known but could be due to in-cage recombination
17 of photoejected PPh₃. The slower kinetics show further bleaching of **1** as the dimer band
18 forms at 1971 cm⁻¹. This is consistent with formation of the dimer by reaction of the fragment
19 [Ru(PPh₃)₂(CO)H₂] with the parent **1** (Figure 12c,d).
20
21
22
23
24
25
26
27
28

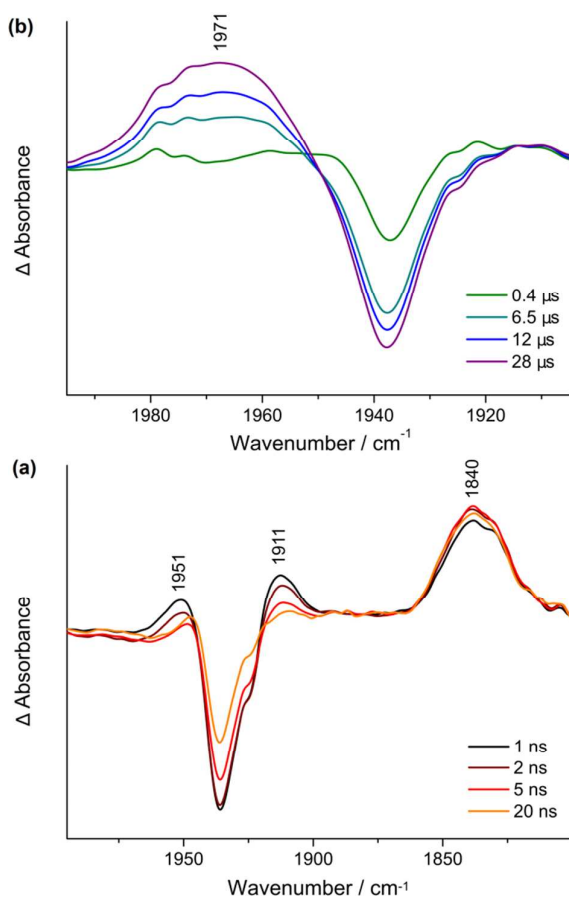


Figure 11. TRIR difference spectra obtained in the range (a) 1-20 ns and 1900-2000 cm^{-1} ; and (b) 0.4-28 μs and 1800-2000 cm^{-1} , after 355 nm laser flash of a solution of **1** in C_6D_6 under an atmosphere of argon.

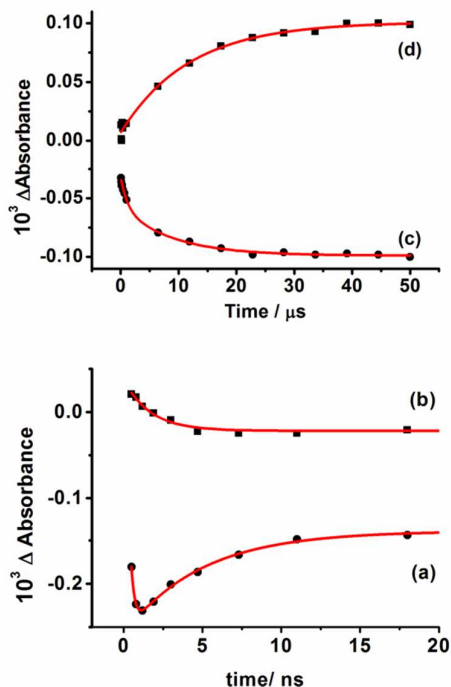


Figure 12. Kinetic plots observed after photolysis of **1** under Ar. Plots a and b on nanosecond timescale, plots c and d on microsecond timescale. (a) 1939 cm^{-1} assigned to **1** which shows a rapid increase, followed by a bleach recovery, $\tau = 4.8 \pm 0.4$ ns; (b) 1951 cm^{-1} , $\tau = 1.7 \pm 0.4$ ns, (c) 1938 cm^{-1} assigned to **1**, $\tau_1 = 1.1 \pm 0.4$ μs , $\tau_2 = 9 \pm 2$ μs and (d) 1970 cm^{-1} assigned to the dimeric species, $\tau = 12 \pm 2$ μs . Δ Absorbances have been normalized.

TRIR of **1 under H_2 in C_6D_6 .** Irradiation of a solution of **1** in the presence of H_2 (1 atm) displays, at early time (Figure 13a), a negative band for **1** and new product bands to both higher and lower frequency of the parent. In agreement with the previous results, the formation of $[\text{Ru}(\text{PPh}_3)_3(\text{CO})]$ at 1840 cm^{-1} is also observed within the time resolution of 0.5 ns; the transient $[\text{Ru}(\text{PPh}_3)_3(\text{CO})]$ was stable up to 28 ns. A product band at 1911 cm^{-1} was formed within 1 ns which decayed with time constant 4.5 ± 0.5 ns and the bleach recovered partially with a time constant 3.0 ± 0.5 ns (Figure 14). The spectrum under H_2 at later times, $\Delta t = 20$ μs , (Figure 13b) superficially resembles the spectrum obtained under argon; however, close inspection shows that the broad band at ~ 1971 cm^{-1} is much more intense relative to the parent bleach in the spectrum under hydrogen. Furthermore, the band at 1971 cm^{-1} grew in significantly faster (ca. 700 ns) under hydrogen compared to the results obtained under argon (ca. 11 μs). These results are consistent with the formation of **2** and its

isomers as a result of the reaction of $[\text{Ru}(\text{PPh}_3)_2(\text{CO})(\text{H})_2]$ with dihydrogen after PPh_3 loss. The formation of some of the dimeric ruthenium species under these conditions cannot be excluded since the $\nu(\text{CO})$ bands of **2** and the dimeric species have been shown to overlap in low temperature FTIR experiments above.

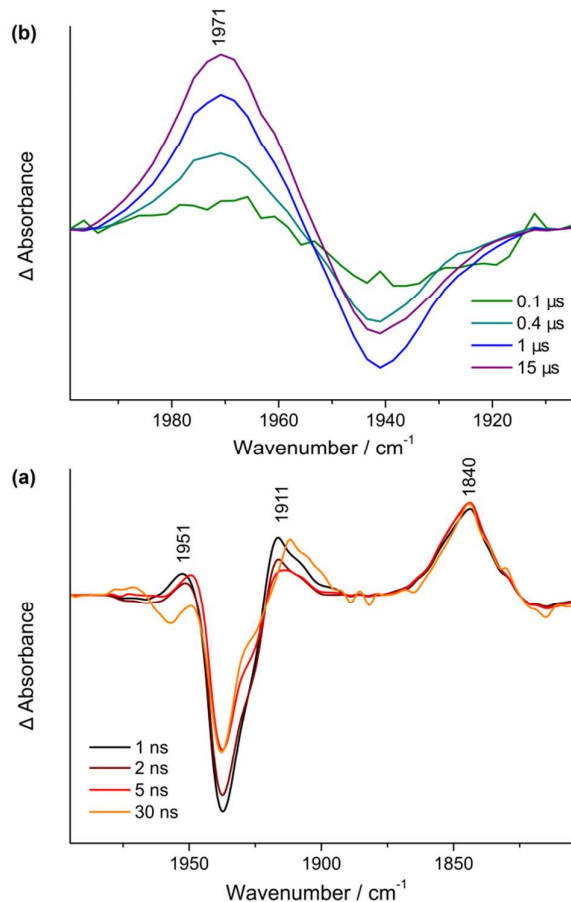


Figure 13. TRIR difference spectra obtained in the range (a) 1-30 ns and $1900\text{-}2000\text{ cm}^{-1}$; and (b) 0.1-15 μs and $1800\text{-}2000\text{ cm}^{-1}$ after 355 nm laser flash of a solution of **1** in C_6D_6 under H_2 (ca. 1.5 atm).

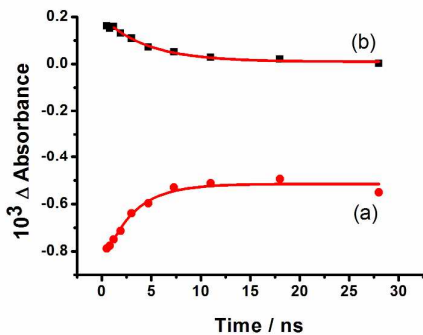
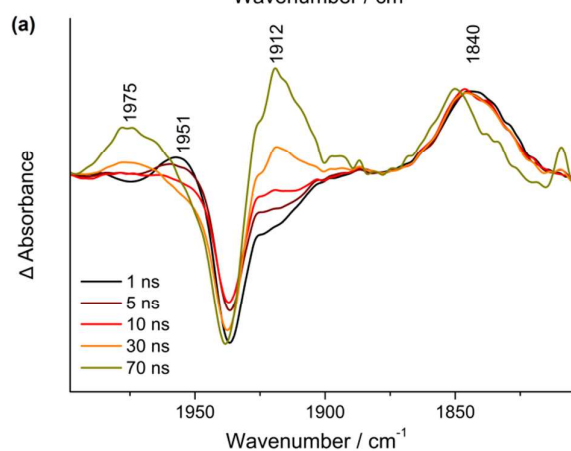
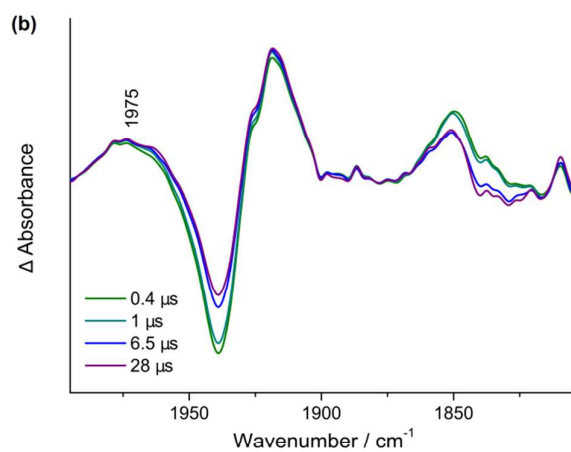


Figure 14. Kinetic plots at early times for (a) bleach recovery of **1** at 1938 cm^{-1} , $\tau = 3.0 \pm 0.5$ ns; (b) loss of 1911 cm^{-1} band assigned to $[\text{Ru}(\text{CO})(\text{PPh}_3)_2(\text{H})_2]$, $\tau = 4.5 \pm 0.5$ ns.

1
2
3
4 **TRIR of 1 in the presence of added pyridine under Ar.** The TRIR spectra obtained
5 after 355 nm irradiation solution of **1** in C_6D_6 with added pyridine (ca. 10^{-2} M) do not show the
6 presence of the band at 1971 cm^{-1} indicating that neither the dimeric product nor **2** are
7 formed under these conditions. However, a clear band at $1915\text{-}1920\text{ cm}^{-1}$ with shoulders
8 both to lower and higher wavenumbers grows in over 100 ns and is assigned to complex **4-CN**
9 or its isomers arising from the reaction of $[Ru(PPh_3)_2(CO)(H)_2]$ with pyridine. This band
10 remains unchanged out to $28\text{ }\mu\text{s}$ (see Supporting Information).

11
12
13
14
15 **TRIR of 1 in the presence of added pyridine under H_2 .** The TRIR spectra obtained
16 after irradiation at 355 nm of a solution of **1** in C_6D_6 with added pyridine (ca. 10^{-2} M) under a
17 H_2 pressure (ca. 1 atm) showed a negative band for **1** at the earliest time (0.5 ns) and a band
18 of $[Ru(PPh_3)_3(CO)]$ as observed in all the earlier experiments. Additionally, the band at 1951 cm^{-1}
19 is detected at early times. Two new bands grew in over 70 ns at 1912 cm^{-1} and 1975 cm^{-1}
20 (Figure 15a). The band at 1912 cm^{-1} is assigned to the formation of complex **4-PP** or
21 isomers while the remaining band coincides with those of complex **2** and the dimer. The
22 band at 1840 cm^{-1} decreases and gives way to a band at 1851 cm^{-1} which may be assigned
23 to $Ru(PPh_3)_3(CO)(py)$. On a longer timescale, these bands are stable (Figure 15b).



1
2
3
4 **Figure 15.** TRIR difference spectra obtained in the range (a) 1-70 ns and 1800-2000 cm^{-1} (b)
5 0.4 - 28 μs after 355 nm laser flash of a solution of **1** in C_6D_6 with added pyridine (ca. 10^{-2} M)
6 under 1 atm H_2 .
7

8 **Discussion**

9
10 The NMR results discussed above differ from our earlier studies in that we see
11 evidence for photochemical loss of both H_2 and of PPh_3 . In the presence of H_2 we see
12 formation of dihydrogen complex **2** while in the presence of triphenylarsine we observe
13 formation of **3**. Use of pyridine as the incoming ligand yields **4-CN** and its isomers. The low
14 temperature FTIR and room temperature TRIR experiments show both intermediates and
15 products consistent with this evidence.
16
17

18 **NMR results.** The behavior of the pyridine isomers is unusual; it might be expected
19 that the initial product would be **4-CN** with *trans* PPh_3 ligands, but the major product at low
20 temperature is **4-PP**. Formation of **4-PP** requires dissociation of PPh_3 and rearrangement of
21 the 5-coordinate intermediate $[\text{Ru}(\text{H})_2(\text{CO})(\text{PPh}_3)_2]$ to bring the PPh_3 ligands into a *cis*
22 orientation. The rearrangement is likely to take place either in an electronic excited state or
23 in a vibrational excited state, as has been documented in detail for $\text{Fe}(\text{CO})_4$ and
24 $\text{Cr}(\text{CO})_5$.^{14,50-55} Initial loss of PPh_3 *trans* to hydride followed by two successive Berry
25 pseudorotations and coordination of pyridine would generate **4-PP**. The surprising feature is
26 that this process is selective for **4-PP**. The isomer **4-PP** rearranges thermally to **4-CN**. Two
27 further isomers of the pyridine complexes **4-NP** and **4-CP** are formed as minor
28 photoproducts. All the isomers are accessible by a single trigonal twist starting from **4-PP**
29 (see Supporting Information).^{56,57} Alternatively, they may occur by isomerization to a
30 dihydrogen complex, followed by a Berry pseudo-rotation.
31
32
33
34
35
36
37

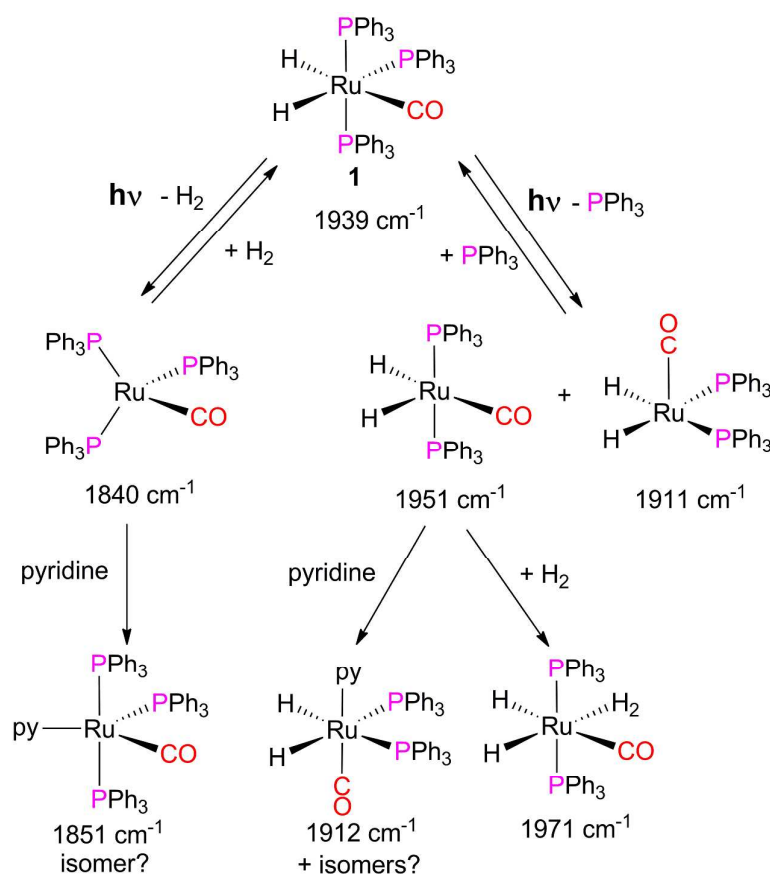
38 It may be asked why parallel isomerization processes are not observed for **2** and **3**. In
39 the case of **2**, we have evidence for rapid exchange of dihydride and dihydrogen ligands
40 which causes rapid conversion to the most stable isomer. For **3**, there is evidence for two
41 further isomers on irradiation with multiple laser shots that are analogues of **4-NP** and **4-CP**
42 (see Supporting Information), but the experiments are limited by the solubility of AsPh_3 at
43 low temperature.
44
45
46

47 The observation of hyperpolarized hydride ligand signals for **3** and **4** on photolysis
48 requires both the substitution of PPh_3 by incoming ligand and reductive elimination of H_2
49 followed by oxidative addition of *p*- H_2 . Considering the short lifetime of hyperpolarized **1**, it is
50 likely that PPh_3 substitution occurs first. We have shown that **3** and **4** undergo thermal
51 exchange with *p*- H_2 and they may also undergo photochemical exchange. The mechanism
52 of this thermal exchange may involve loss of AsPh_3 or pyridine from **3** or **4**, respectively,
53 followed by formation of **2**, intramolecular exchange of hydrogens and recoordination of
54
55
56
57
58
59
60

ligand, as proposed for related iridium complexes.⁵⁸ Alternatively and more simply, **3** and **4** may be converted to dihydrogen isomers which undergo exchange with *p*-H₂ and regeneration of the initial structure.

IR results. The IR spectra and reactivity of the Ru(0) intermediate, [Ru(PPh₃)₃(CO)], are consistent with a single isomer of this species. On the other hand, the IR spectra point to the formation of at least two isomers of the Ru(II) intermediate [Ru(H)₂(CO)(PPh₃)₂] (Scheme 6).

Scheme 6. Summary of TRIR observations with experimental IR wavenumbers for $\nu(\text{CO})$



We have investigated the assignments further by use of Timney ligand effect constants⁵⁹ and by estimating the CO stretching frequencies by DFT methods (Table 1). The ligand effect constant for PPh₃ *cis* to CO is negative while that for *trans*-PPh₃ is positive; thus values of $\nu(\text{CO})$ will be very sensitive to the OC–Ru–P angle. The values for hydride are positive for both *cis* and *trans* geometries and greatly exceed the values for the other ligands. The Timney calculations are consistent with a butterfly structure for [Ru(PPh₃)₃CO] and two isomers of square pyramidal [Ru(CO)(PPh₃)₂(H)₂]. Loss of PPh₃ *trans* to hydride without rearrangement of the skeleton of **1** should cause a high frequency shift in $\nu(\text{CO})$ with

respect to **1**, whereas rearrangement to an isomer with mutually *cis* hydrides and CO *trans* to a vacancy should cause a shift lower frequency than that of **1**. The corresponding DFT calculations are summarized in Table 1. In light of these calculations, we deduce that PPh₃ photo-ejection does indeed generate two isomers of [Ru(H)₂(CO)(PPh₃)₂].

The $\nu(\text{CO})$ band of dihydrogen complex **2** is reproduced very accurately by both calculation methods; the high frequency shift is consistent with the expected π -acceptor characteristics. The values for pyridine complexes **4-CN** and **4-PP** pose greater problems (see SI).

The intermediate [Ru(H)₂(CO)(PPh₃)₂] is much more reactive than [Ru(PPh₃)₃(CO)] and we anticipate that it will react with incoming substrates to generate isomeric products. The nanosecond TRIR spectra showed strong evidence for partial in-cage recombination of PPh₃ with [Ru(H)₂(CO)(PPh₃)₂] with time constant of ca. 5 ns. The reaction of this species with H₂ under 1.5 atm (the solubility of H₂ in benzene is $2.9 \times 10^{-3} \text{ mol dm}^{-3} \text{ atm}^{-1}$)⁶⁰ took place with $\tau \sim 700$ ns, while the reaction with pyridine occurred with $\tau \sim 70$ ns at $10^{-2} \text{ mol dm}^{-3}$ pyridine, indicating considerably higher reactivity toward pyridine than toward H₂. The reaction of [Ru(PPh₃)₃(CO)] with H₂ is considerably slower (τ ca. 3 μs at the same pressure).

Table 1. Wavenumbers of $\nu(\text{CO})$ bands/cm⁻¹

Complex	$\nu(\text{CO})$ exptl in C ₆ D ₆	$\nu(\text{CO})$ calcd by Timney method ^a	$\nu(\text{CO})$ calcd by DFT ^b
1	1939	1947	1927
2	1971	1971	1974
spy Ru(H) ₂ (CO)(PPh ₃) ₂ vacancy <i>trans</i> to H ^c	1951	1960	1973
spy Ru(H) ₂ (CO)(PPh ₃) ₂ vacancy <i>trans</i> to CO ^c	1911	1925	
Ru(CO)(PPh ₃) ₃ sq planar ^c	1840	1923	
Ru(CO)(PPh ₃) ₃ butterfly	1840	1842	1903

^a Reference ⁵⁹

^b M06/LACVP(d) with 0.96 scaling

^c spy = square pyramidal; sq = square

Conclusions

The evidence from *in-situ* photochemistry of **1** with both NMR and IR detection that PPh₃ loss competes with H₂ reductive elimination is very strong indeed. When we first obtained

1
2
3 NMR evidence for PPh₃ substitution by H₂ to form Ru(H)₂(η²-H₂)(CO)(PPh₃)₂ **2**, the
4 experiments seemed to conflict with our earlier TRIR experiments.¹⁵ However with the
5 improved performance of modern TRIR experiments, it is now evident that we missed this
6 reaction because of the need for NMR spectroscopy at low temperature and TRIR
7 spectroscopy with greater sensitivity and time resolution. Our NMR experiments indicate that
8 the quantum yields for PPh₃ loss and H₂ reductive elimination are approximately equal on
9 355 nm photolysis.

10
11
12
13 The TRIR experiments allow characterization of coordinatively unsaturated
14 [Ru(PPh₃)₃(CO)] and two isomers of [Ru(H)₂(CO)(PPh₃)₂] via their ν(CO) bands. They also
15 demonstrate that [Ru(H)₂(CO)(PPh₃)₂] is considerably more reactive toward H₂ than
16 [Ru(PPh₃)₃(CO)]. The reaction of [Ru(PPh₃)₃(CO)] with *p*-H₂ generates **1** in hyperpolarized
17 form, but this species relaxes fast and does not exchange with *p*-H₂ and consequently can
18 only be detected if the laser pulse is synchronized with the *r.f.* pulse from the NMR
19 spectrometer. The reaction of [Ru(H)₂(CO)(PPh₃)₂] with H₂ generates the dihydrogen
20 complex Ru(H)₂(η²-H₂)(CO)(PPh₃)₂ **2**. Its short T₁ provides a route to relaxation of *p*-H₂ to
21 thermal equilibrium of *o*-H₂ and *p*-H₂; however, its formation and the fast relaxation process
22 can be suppressed by addition of other ligands. Reaction of AsPh₃ in the presence of *p*-H₂
23 generates hyperpolarized Ru(H)₂(AsPh₃)(CO)(PPh₃)₂ **3**. The reaction of [Ru(H)₂(CO)(PPh₃)₂]
24 with pyridine is more complex. Use of low temperature methods shows that the initial product
25 is Ru(H)₂(CO)(PPh₃)₂(pyridine) **4-PP** with a planar Ru(H)₂(PPh₃)₂ core and pyridine *trans* to
26 CO. This species rearranges on warming to **4-CN**, the pyridine analogue of complexes **2** and
27 **3**. Two more isomers, **4-NP** and **4-CP**, are formed in low yield. Under an atmosphere of *p*-
28 H₂, all four isomers are detected in hyperpolarized form. Unlike **1**, complexes **3** and **4-CN**
29 undergo thermal exchange at room temperature with *p*-H₂.

30 31 32 33 34 35 36 37 38 39 40 41 42 43 44 45 46 47 48 49 50 51 52 53 54 55 56 57 58 59 60

Experimental Section

Complex **1** was prepared using the old procedure reported in the literature.⁶¹ Chemical
manipulations and sample preparations were carried out under inert atmosphere conditions
using standard Schlenk (vacuum 10⁻² mbar) or high vacuum (10⁻⁴ mbar). *p*-H₂ was generated
by cooling hydrogen gas over charcoal in a copper block at ca. 30 K. The proportion of *p*-H₂
at 30 K was calculated as > 99%. Pressures of *p*-H₂ were measured with an MKS Baratron
capacitance manometer. Deuterated solvents for use in NMR were degassed and dried
before use; benzene-*d*₆ and toluene-*d*₈ were obtained from Aldrich and dried on potassium
mirrors in ampoules fitted with a greaseless tap. ¹⁵N-pyridine (Aldrich) was used as received.

NMR measurements. Ex-situ UV photolysis setup. Photochemical reactions were
performed with an Oriel 350 Watt high pressure xenon arc. Unwanted heating was
minimized by use of a water filter of 10 cm length between the sample and the lamp.

1
2
3 **Continuous wave laser experiments.** The *in-situ* photolysis equipment has been
4 described before.⁶² In summary, *in-situ* photolysis experiments were performed using a
5 wide-bore Bruker DRX-400 NMR spectrometer equipped with a 63 mW Kimmon IK series
6 He-Cd laser at 325 nm. The laser beam is directed into the sample in the spectrometer
7 through the air-gap between the magnet bore and a narrow-bore probe. The sample is
8 cooled using a liquid N₂ boil-off evaporator. The laser was mounted on a specially designed
9 platform situated in front of the NMR spectrometer that could be adjusted both horizontally
10 and vertically. The laser alignment was optimized by using an NMR sample of
11 Ru(CO)₃(dppe) (dppe = Ph₂PCH₂CH₂PPh₂) in deuterated toluene, pressurized with *p*-H₂.
12 When exposed to UV light the sample reacts with *p*-H₂ to generate enhanced resonances
13 arising from Ru(H)₂(CO)₃(dppe). Continuous recording of the spectra allowed the optimal
14 position of the laser beam to be identified.
15
16

17 **Pulsed laser experiments.** All NMR spectra were recorded on a Bruker Avance II 600
18 MHz spectrometer with a 14 T wide-bore magnet fitted with a 5 mm BBO probe. In situ laser
19 photolysis was carried out with a pulsed Nd:YAG laser (Continuum Surelite II) fitted with a
20 frequency tripling crystal (output 355 nm). Operating conditions were typically: 10 Hz
21 repetition rate, flash lamp voltage 1.49 kV, and Q-switch delay increased from the standard
22 to 320 μs yielding a laser power of 75 mW in internal mode. The energy of a single laser
23 pulse was measured using an energy meter calibrated for 355 nm to be ~ 29.8 mJ at our
24 operating conditions (external triggering with Q-switch delay set to 150 μs). The unfocused
25 laser beam is directed at the base of the spectrometer and reflected up into the probe *via*
26 a mirror as previously reported.³² Adjustment screws control the vertical and horizontal
27 position of the mirror which is on a kinematic mount. The system is fully shielded from the
28 operator and the screws of the kinematic mount can be adjusted from outside the shield. The
29 laser radiation is incident on a fixed mirror that is level with the sample and passes through a
30 hole in the probe onto the NMR tube. Standard NMR tubes fitted with Young's taps were
31 used. The samples contained 1–2 mg of compound (Abs₃₅₅ ~ 0.7) and approximately 0.4 mL
32 of solvent. A sample of Ru(dppe)₂H₂ in C₆D₆ was used for laser alignment with *p*-H₂
33 amplification in real time. Standard NMR pulse sequences were modified for use with *p*-H₂
34 by including a synchronized laser initiation sequence prior to NMR excitation. A purpose-
35 written program was used to control the laser firing from the NMR console with the laser set
36 on external triggering. The program sets the laser to fire one warm-up shot before the fire
37 signal. The NMR pulse is initiated at a set delay time (τ) following the fire signal. The intrinsic
38 time delay between sending the fire signal from the spectrometer and the actual firing of the
39 laser pulse was measured with a photodiode and an oscilloscope to be 150 μs (equal to the
40 Q-switch delay for the generation of the pulse). This signal delay was incorporated into the
41
42
43
44
45
46
47
48
49
50
51
52
53
54
55
56
57
58
59
60

1
2
3 pulse sequence such that synchronized measurements with a time delay, τ , were achieved
4 by setting the spectrometer delay to: $\tau + 150 \mu\text{s}$. The precision of this delay between the
5 laser and radio frequency (*r.f.*) pulses is controlled by the 200 ns clock of the spectrometer.
6

7 **TRIR measurements.** Our time-resolved infrared (TRIR) measurements were based
8 on pump-probe method that has been described in detail previously.^{30,63} In brief, the probe
9 source is a broadband mid-IR pulse with 100 fs duration (fwhm) and around 1 μJ energy at 1
10 kHz. The pump source is the third harmonic output (355 nm) of a Q-switched Nd:YVO laser
11 with 0.5 ps duration (fwhm) and around 3 μJ energy and is synchronized to the probe pulse.
12 The delay between pump and probe pulses can be controlled with a pulse generator
13 (DG535, Stanford Research System) from 0.5 ns to 100 μs . The broadband transmitted
14 probe pulse is detected with a 128-element HgCdTe array detector. The sample solutions
15 were flowed through a CaF_2 windowed IR cell, path length (0.25 mm), which was rastered in
16 two dimensions at high speed to reduce overheating and degradation of the sample solution.
17 All spectral and kinetic fitting procedures were carried out using Microcal Origin 7 software.
18

19 **Low Temperature Photolysis.** The low temperature photolysis IR experiments were
20 performed in a similar manner to those described previously.⁶⁴ The high pressure-low
21 temperature (HP-LT) cell used in the low temperature experiments has been described in
22 detail elsewhere.⁶⁵ Briefly, the HP-LT cell was filled with a solution of **1** dissolved in toluene-
23 d_8 . Toluene- d_8 was used to minimize IR solvent background issues and to permit low
24 temperature experiments in solution because of its lower freezing point than that of benzene-
25 d_6 . The cell was attached to a cold finger of a cryogenic cooling system and cooled to the
26 required temperature (220 K). The photolysis source used in these experiments was a
27 Philips HPK 125W medium-pressure mercury arc lamp, which provided broadband UV and
28 visible light. IR spectra were recorded using a Nicolet 730 interferometer linked to a
29 computer running Omnic software.
30

31 **IR spectroscopy.** Other IR spectra were recorded on a Mattson Unicam RS FTIR
32 instrument, connected to a PC running WINFIRST software, or a Nicolet Nexus, connected
33 to a PC running Omnic E.S.P. 5.2 software.
34

35 **UV-Vis spectroscopy.** UV-Vis spectra were recorded on a Perkin-Lambda 7
36 spectrometer, using a PC running PECSS software.
37

38 **DFT calculations.** Density functional theory calculations were used to optimize
39 geometries and simulate harmonic vibrational frequencies for several of the complexes (see
40 Supporting information). Preliminary calculations of the parent species performed with the
41 Stuttgart relativistic small core pseudopotential and basis set mixed with the 6-311G(d) basis
42 set for non-metal atoms,⁶⁶ and using the B3LYP^{67,68} PBE0,⁶⁹ and M06⁷⁰ functionals,
43 representing 20, 25, and 27 % HF exchange, respectively, found that M06 gave the closest
44
45
46
47
48
49
50
51
52
53
54
55
56
57
58
59
60

1
2
3 match with experiment. Consequently, the M06 level of theory within the Q-Chem quantum-
4 chemical software package was adopted for fuller calculations.⁷¹ Calculations were
5 converged then using the double- ζ 6-31G(d) basis set for C, N, O, P, and H atoms, and the
6 quasi-relativistic LANL2DZ pseudo-potential and basis set for Ru.⁷² This combination has
7 been labelled as LACVP(d). Optimized geometries were confirmed by the absence of
8 imaginary frequencies, and these harmonic frequencies have been scaled by a uniform
9 factor of 0.96 to account for anharmonic and experimental effects.⁷³
10
11
12

13 **ASSOCIATED CONTENT**

14 **Supporting Information**

15
16 The Supporting Information is available free of charge on the ACS Publications website at
17 DOI: 10.1021/acs/organomet.xxxxx
18

19 NMR spectra, pulse sequences used in laser pump-NMR probe experiments, $T_{1(\text{min})}$
20 relaxation, TRIR difference spectra, FTIR spectra, DFT calculated structures and CO-
21 stretching frequencies, calculated and observed $\nu(\text{CO})$ values for pyridine complexes.
22
23
24

25 **AUTHOR INFORMATION**

26 **Corresponding Authors**

27 *E-mail for S.B.D.: simon.duckett@york.ac.uk

28 *E-mail for M.W.G.: mike.george@nottingham.ac.uk

29 *E-mail for R.N.P.: robin.perutz@york.ac.uk
30
31

32 **ORCID**

33 Simon B. Duckett: 0000-0002-9788-6615

34 Michael W. George: 0000-0002-7844-1696

35 Robin N. Perutz: 0000-0001-6286-0282

36 Barbara Procacci: 0000-0001-7044-0560

37 Magnus Hanson-Heine 0000-0002-6709-297X

38 Raphael Horvath 0000-0002-2695-4895

39 Khuong Vuong 0000-0001-9558-9273
40
41
42
43

44 **Notes**

45 The authors declare no competing financial interest.
46
47

48 **ACKNOWLEDGEMENTS**

49 We are grateful for financial support from EPSRC (grants EP/K022792/1 and EP/D058031).
50 We acknowledge assistance from Dr. Pedro Aguiar. MWG gratefully acknowledges receipt
51 of a Wolfson Merit Award.
52
53

54 **REFERENCES**

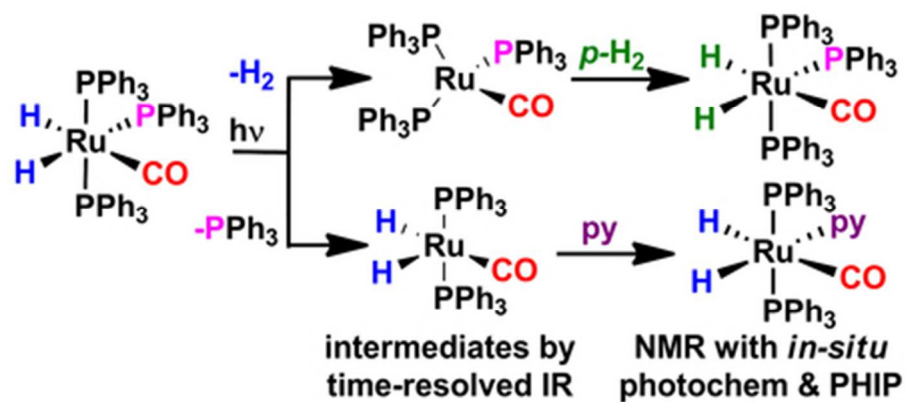
55
56
57
58
59
60

- 1
- 2
- 3 (1) Crossley, S. W. M.; Obradors, C.; Martinez, R. M.; Shenvi, R. A. *Chem. Rev.* **2016**,
- 4 *116*, 8912-9000.
- 5
- 6 (2) Maity, A.; Teets, T. S. *Chem. Rev.* **2016**, *116*, 8873-911.
- 7
- 8 (3) Rossin, A.; Peruzzini, M. *Chem. Rev.* **2016**, *116*, 8848-72.
- 9
- 10 (4) Perutz, R. N.; Procacci, B. *Chem. Rev.* **2016**, *116*, 8506-44.
- 11
- 12 (5) Geoffroy, G. L.; Bradley, M. G. *Inorg. Chem.* **1977**, *16*, 744-8.
- 13
- 14 (6) Wakatsuki, Y.; Yamazaki, H.; Kumegawa, N.; Satoh, T.; Satoh, J. Y. *J. Am. Chem.*
- 15 *Soc.* **1991**, *113*, 9604-10.
- 16
- 17 (7) Wakatsuki, Y.; Yamazaki, H.; Maruyama, Y.; Shimizu, I. *J. Chem. Soc., Chem.*
- 18 *Commun.* **1991**, 261-3.
- 19
- 20 (8) Du, H. G.; Liu, Q.; Shi, S. J.; Zhang, S. W. *J. Organomet. Chem.* **2001**, *627*, 127-31.
- 21
- 22 (9) Samouei, H.; Grushin, V. V. *Organometallics* **2013**, *32*, 4440-3.
- 23
- 24 (10) Arockiam, P. B.; Bruneau, C.; Dixneuf, P. H. *Chem. Rev.* **2012**, *112*, 5879-918.
- 25
- 26 (11) Kakiuchi, F.; Murai, S. *Acc. Chem. Res.* **2002**, *35*, 826-34.
- 27
- 28 (12) Nixon, T. D.; Whittlesey, M. K.; Williams, J. M. J. *Dalton Trans.* **2009**, 753-62.
- 29
- 30 (13) Naota, T.; Takaya, H.; Murahashi, S. I. *Chem. Rev.* **1998**, *98*, 2599-660.
- 31
- 32 (14) Perutz, R. N.; Torres, O.; Vlček, A. J. *Photochemistry of Metal Carbonyls,*
- 33 *Comprehensive Inorganic Chemistry II Reedijk, J., Poeppelmeier, K., Eds.; Elsevier: Oxford,*
- 34 *U.K., 2013; Vol. 8, Ch. 8.06* **2013**, 229-53.
- 35
- 36 (15) Colombo, M.; George, M. W.; Moore, J. N.; Pattison, D. I.; Perutz, R. N.; Virrels, I. G.;
- 37 Ye, T. Q. *J. Chem. Soc., Dalton Trans.* **1997**, 2857-9.
- 38
- 39 (16) Torres, O.; Calladine, J. A.; Duckett, S. B.; George, M. W.; Perutz, R. N. *Chem. Sci.*
- 40 **2015**, *6*, 418-24.
- 41
- 42 (17) Calladine, J. A.; Torres, O.; Anstey, M.; Ball, G. E.; Bergman, R. G.; Curley, J.;
- 43 Duckett, S. B.; George, M. W.; Gilson, A. I.; Lawes, D. J.; Perutz, R. N.; Sun, X. Z.; Vollhardt,
- 44 K. P. C. *Chem. Sci.* **2010**, *1*, 622-30.
- 45
- 46 (18) Calladine, J. A.; Duckett, S. B.; George, M. W.; Matthews, S. L.; Perutz, R. N.;
- 47 Torres, O.; Khuong, Q. V. *J. Am. Chem. Soc.* **2011**, *133*, 2303-10.
- 48
- 49 (19) Godard, C.; Callaghan, P.; Cunningham, J. L.; Duckett, S. B.; Lohman, J. A. B.;
- 50 Perutz, R. N. *Chem. Commun.* **2002**, 2836-7.
- 51
- 52 (20) Blazina, D.; Dunne, J. P.; Aiken, S.; Duckett, S. B.; Elkington, C.; McGrady, J. E.;
- 53 Poli, R.; Walton, S. J.; Anwar, M. S.; Jones, J. A.; Carteret, H. A. *Dalton Trans.* **2006**, 2072-
- 54 80.
- 55
- 56 (21) Gefதாக, S.; Ball, G. E. *J. Am. Chem. Soc.* **1998**, *120*, 9953-4.
- 57
- 58 (22) Lawes, D. J.; Gefதாக, S.; Ball, G. E. *J. Am. Chem. Soc.* **2005**, *127*, 4134-5.
- 59
- 60 (23) Ball, G. E.; Brookes, C. M.; Cowan, A. J.; Darwish, T. A.; George, M. W.; Kawanami,
- H. K.; Portius, P.; Rourke, J. P. *Proc. Natl. Acad. Sci.* **2007**, *104*, 6927-32.

- 1
2
3 (24) Lawes, D. J.; Darwish, T. A.; Clark, T.; Harper, J. B.; Ball, G. E. *Angew. Chem., Int.*
4 *Ed.* **2006**, *45*, 4486-90.
5
6 (25) Young, R. D.; Hill, A. F.; Hillier, W.; Ball, G. E. *J. Am. Chem. Soc.* **2011**, *133*, 13806-
7 9.
8
9 (26) Ampt, K. A. M.; Burling, S.; Donald, S. M. A.; Douglas, S.; Duckett, S. B.; Macgregor,
10 S. A.; Perutz, R. N.; Whittlesey, M. K. *J. Am. Chem. Soc.* **2006**, *128*, 7452-3.
11
12 (27) Montiel-Palma, V.; Perutz, R. N.; George, M. W.; Jina, O. S.; Sabo-Etienne, S.
13 *Chem. Commun.* **2000**, 1175-6.
14
15 (28) Calladine, J. A.; Horvath, R.; Davies, A. J.; Wriglesworth, A.; Sun, X. Z.; George, M.
16 *W. Appl. Spectrosc.* **2015**, *69*, 519-24.
17
18 (29) Greetham, G. M.; Burgos, P.; Cao, Q. A.; Clark, I. P.; Codd, P. S.; Farrow, R. C.;
19 George, M. W.; Kogimtzis, M.; Matousek, P.; Parker, A. W.; Pollard, M. R.; Robinson, D. A.;
20 Xin, Z. J.; Towrie, M. *Appl. Spectrosc.* **2010**, *64*, 1311-9.
21
22 (30) Towrie, M.; Grills, D. C.; Dyer, J.; Weinstein, J. A.; Matousek, P.; Barton, R.; Bailey,
23 P. D.; Subramaniam, N.; Kwok, W. M.; Ma, C. S.; Phillips, D.; Parker, A. W.; George, M. W.
24 *Appl. Spectrosc.* **2003**, *57*, 367-80.
25
26 (31) Banister, J. A.; George, M. W.; Grubert, S.; Howdle, S. M.; Jobling, M.; Johnson, F.
27 P. A.; Morrison, S. L.; Poliakoff, M.; Schubert, U.; Westwell, J. R. *J. Organomet. Chem.*
28 **1994**, *484*, 129-35.
29
30 (32) Torres, O.; Procacci, B.; Halse, M. E.; Adams, R. W.; Blazina, D.; Duckett, S. B.;
31 Eguillor, B.; Green, R. A.; Perutz, R. N.; Williamson, D. C. *J. Am. Chem. Soc.* **2014**, *136*,
32 10124-31.
33
34 (33) Pravdivtsev, A. N.; Yurkovskayaa, A. V.; Petrov, P. A.; Vieth, H. M. *Phys. Chem.*
35 *Chem. Phys.* **2017**, *19*, 25961-69.
36
37 (34) Levison, J. J. *J. Chem. Soc. A* **1970**, 639-43.
38
39 (35) Perutz, R. N.; Sabo-Etienne, S. *Angew. Chem., Int. Ed.* **2007**, *46*, 2578-92.
40
41 (36) Luo, X. L.; Crabtree, R. H. *J. Am. Chem. Soc.* **1990**, *112*, 6912-8.
42
43 (37) Crabtree, R. H. *Chem. Rev.* **2016**, *116*, 8750-69.
44
45 (38) Gusev, D. G.; Vymenits, A. B.; Bakhmutov, V. I. *Inorg. Chim. Acta* **1991**, *179*, 195-
46 201.
47
48 (39) Samouei, H.; Miloserdov, F. M.; Escudero-Adan, E. C.; Grushin, V. V.
49 *Organometallics* **2014**, *33*, 7279-83.
50
51 (40) Riddlestone, I. M.; McKay, D.; Gutmann, M. J.; Macgregor, S. A.; Mahon, M. F.;
52 Sparkes, H. A.; Whittlesey, M. K. *Organometallics* **2016**, *35*, 1301-12.
53
54 (41) Grellier, M.; Mason, S. A.; Albinati, A.; Capelli, S. C.; Rizzato, S.; Bijani, C.; Coppel,
55 Y.; Sabo-Etienne, S. *Inorg. Chem.* **2013**, *52*, 7329-37.
56
57
58
59
60

- 1
2
3 (42) Hebden, T. J.; Goldberg, K. I.; Heinekey, D. M.; Zhang, X. W.; Emge, T. J.; Goldman,
4 A. S.; Krogh-Jespersen, K. *Inorg. Chem.* **2010**, *49*, 1733-42.
5
6 (43) Morris, R. H. *Coord. Chem. Rev.* **2008**, *252*, 2381-94.
7
8 (44) Sleigh, C. J.; Duckett, S. B.; Mawby, R. J.; Lowe, J. P. *Chem. Commun.* **1999**, 1223-
9 4.
10
11 (45) The dimer observed by TRIR spectroscopy offers a potential route to formation of
12 $\text{Ru}(\text{H})_2(\text{PPh}_3)_2(\text{CO})_2$ see section on IR studies.
13
14 (46) Ball, G. E.; Mann, B. E. *J. Chem. Soc., Chem. Commun.* **1992**, 561-3.
15
16 (47) Aguilar, J. A.; Elliott, P. I. P.; Lopez-Serrano, J.; Adams, R. W.; Duckett, S. B. *Chem.*
17 *Commun.* **2007**, 1183-5.
18
19 (48) Abdur-Rashid, K.; Abbel, R.; Hadzovic, A.; Lough, A. J.; Morris, R. H. *Inorg. Chem.*
20 **2005**, *44*, 2483-92.
21
22 (49) Halse, M. E.; Procacci, B.; Henshaw, S. L.; Perutz, R. N.; Duckett, S. B. *J. Magn.*
23 *Reson.* **2017**, *278*, 25-38.
24
25 (50) Besora, M.; Carreon-Macedo, J. L.; Cimas, A.; Harvey, J. N. *Adv. Inorg. Chem., Vol*
26 *61: Metal Ion Controlled Reactivity* **2009**, *61*, 573-623.
27
28 (51) Kosma, K.; Trushin, S. A.; Fuss, W.; Schmid, W. E.; Schneider, B. M. R. *Phys.*
29 *Chem. Chem. Phys.* **2010**, *12*, 13197-214.
30
31 (52) Trushin, S. A.; Fuss, W.; Kompa, K. L.; Schmid, W. E. *J. Phys. Chem. A* **2000**, *104*,
32 1997-2006.
33
34 (53) Paterson, M. J.; Hunt, P. A.; Robb, M. A.; Takahashi, O. *J. Phys. Chem. A* **2002**, *106*,
35 10494-504.
36
37 (54) Portius, P.; Yang, J. X.; Sun, X. Z.; Grills, D. C.; Matousek, P.; Parker, A. W.; Towrie,
38 M.; George, M. W. *J. Am. Chem. Soc.* **2004**, *126*, 10713-20.
39
40 (55) Burdett, J. K.; Grzybowski, J. M.; Perutz, R. N.; Poliakoff, M.; Turner, J. J.; Turner, R.
41 *F. Inorg. Chem.* **1978**, *17*, 147-54.
42
43 (56) Soubra, C.; Oishi, Y.; Albright, T. A.; Fujimoto, H. *Inorg. Chem.* **2001**, *40*, 620-7.
44
45 (57) Rodger, A.; Johnson, B. F. G. *Inorg. Chem.* **1988**, *27*, 3061-2.
46
47 (58) Ruddlesden, A. J.; Mewis, R. E.; Green, G. G. R.; Whitwood, A. C.; Duckett, S. B.
48 *Organometallics* **2015**, *34*, 2997-3006.
49
50 (59) Timney, J. A. *Inorg. Chem.* **1979**, *18*, 2502-6.
51
52 (60) Wilhelm, E.; Battino, R. *Chem. Rev.* **1973**, *73*, 1-9.
53
54 (61) Ahmad, N.; Uttley, M. F.; Robinson, S. D. *J. Chem. Soc., Dalton Trans.* **1972**, 843-7.
55
56 (62) Clark, J. L.; Duckett, S. B. *Dalton Trans.* **2014**, *43*, 1162-71.
57
58 (63) Brennan, P.; George, M. W.; Jina, O. S.; Long, C.; McKenna, J.; Pryce, M. T.; Sun,
59 X. Z.; Vuong, K. Q. *Organometallics* **2008**, *27*, 3671-80.
60

- 1
2
3 (64) Childs, G. I.; Colley, C. S.; Dyer, J.; Grills, D. C.; Sun, X. Z.; Yang, J. X.; George, M.
4 *W. J. Chem. Soc., Dalton Trans.* **2000**, 1901-6.
5
6 (65) Cooper, A. I.; Poliakoff, M. *Chem. Phys. Lett.* **1993**, 212, 611-6.
7
8 (66) Dolg, M.; Wedig, U.; Stoll, H.; Preuss, H. *J. Chem. Phys.* **1987**, 86, 866-72.
9
10 (67) Becke, A. D. *J. Chem. Phys.* **1993**, 98, 5648-52.
11
12 (68) Stephens, P. J.; Devlin, F. J.; Chabalowski, C. F.; Frisch, M. J. *J. Phys. Chem.* **1994**,
13 98, 11623-7.
14
15 (69) Adamo, C.; Barone, V. *J. Chem. Phys.* **1999**, 110, 6158-70.
16
17 (70) Zhao, Y.; Truhlar, D. G. *Theor. Chem. Acc.* **2008**, 120, 215-41.
18
19 (71) Shao, Y. H.; Gan, Z. T.; Epifanovsky, E.; Gilbert, A. T. B.; Wormit, M.; Kussmann, J.;
20 Lange, A. W.; Behn, A.; Deng, J.; Feng, X. T.; Ghosh, D.; Goldey, M.; Horn, P. R.; Jacobson,
21 L. D.; Kaliman, I.; Khaliullin, R. Z.; Kus, T.; Landau, A.; Liu, J.; Proynov, E. I.; Rhee, Y. M.;
22 Richard, R. M.; Rohrdanz, M. A.; Steele, R. P.; Sundstrom, E. J.; Woodcock, H. L.;
23 Zimmerman, P. M.; Zuev, D.; Albrecht, B.; Alguire, E.; Austin, B.; Beran, G. J. O.; Bernard,
24 Y. A.; Berquist, E.; Brandhorst, K.; Bravaya, K. B.; Brown, S. T.; Casanova, D.; Chang, C.
25 M.; Chen, Y. Q.; Chien, S. H.; Closser, K. D.; Crittenden, D. L.; Diedenhofen, M.; DiStasio,
26 R. A.; Do, H.; Dutoi, A. D.; Edgar, R. G.; Fatehi, S.; Fusti-Molnar, L.; Ghysels, A.; Golubeva-
27 Zadorozhnaya, A.; Gomes, J.; Hanson-Heine, M. W. D.; Harbach, P. H. P.; Hauser, A. W.;
28 Hohenstein, E. G.; Holden, Z. C.; Jagau, T. C.; Ji, H. J.; Kaduk, B.; Khistyayev, K.; Kim, J.;
29 Kim, J.; King, R. A.; Klunzinger, P.; Kosenkov, D.; Kowalczyk, T.; Krauter, C. M.; Lao, K. U.;
30 Laurent, A. D.; Lawler, K. V.; Levchenko, S. V.; Lin, C. Y.; Liu, F.; Livshits, E.; Lochan, R. C.;
31 Luenser, A.; Manohar, P.; Manzer, S. F.; Mao, S. P.; Mardirossian, N.; Marenich, A. V.;
32 Maurer, S. A.; Mayhall, N. J.; Neuscamman, E.; Oana, C. M.; Olivares-Amaya, R.; O'Neill, D.
33 P.; Parkhill, J. A.; Perrine, T. M.; Peverati, R.; Prociuk, A.; Rehn, D. R.; Rosta, E.; Russ, N.
34 J.; Sharada, S. M.; Sharma, S.; Small, D. W.; Sodt, A. *Mol. Phys.* **2015**, 113, 184-215.
35
36 (72) Hay, P. J.; Wadt, W. R. *J. Chem. Phys.* **1985**, 82, 299-310.
37
38 (73) Merrick, J. P.; Moran, D.; Radom, L. *J. Phys. Chem. A* **2007**, 111, 11683-700.
39
40
41
42
43
44
45
46
47
48
49
50
51
52
53
54
55
56
57
58
59
60



graphical abstract

38x17mm (300 x 300 DPI)